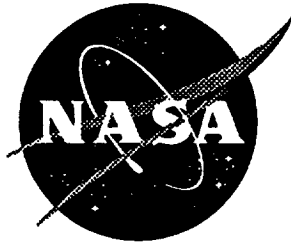


NASA Technical Memorandum 109132



Satellite Estimates of Shortwave Surface Radiation and Atmospheric Meteorology for the BOREAS Experiment Region

C. D. Moats

Lockheed Engineering & Sciences Company, Hampton, Virginia

C. H. Whitlock

Langley Research Center, Hampton, Virginia

S. R. LeCroy and R. C. DiPasquale

Lockheed Engineering & Sciences Company, Hampton, Virginia

(NASA-TM-109132) SATELLITE
ESTIMATES OF SHORTWAVE SURFACE
RADIATION AND ATMOSPHERIC
METEOROLOGY FOR THE BOREAS
EXPERIMENT REGION (NASA, Langley
Research Center) 57 p

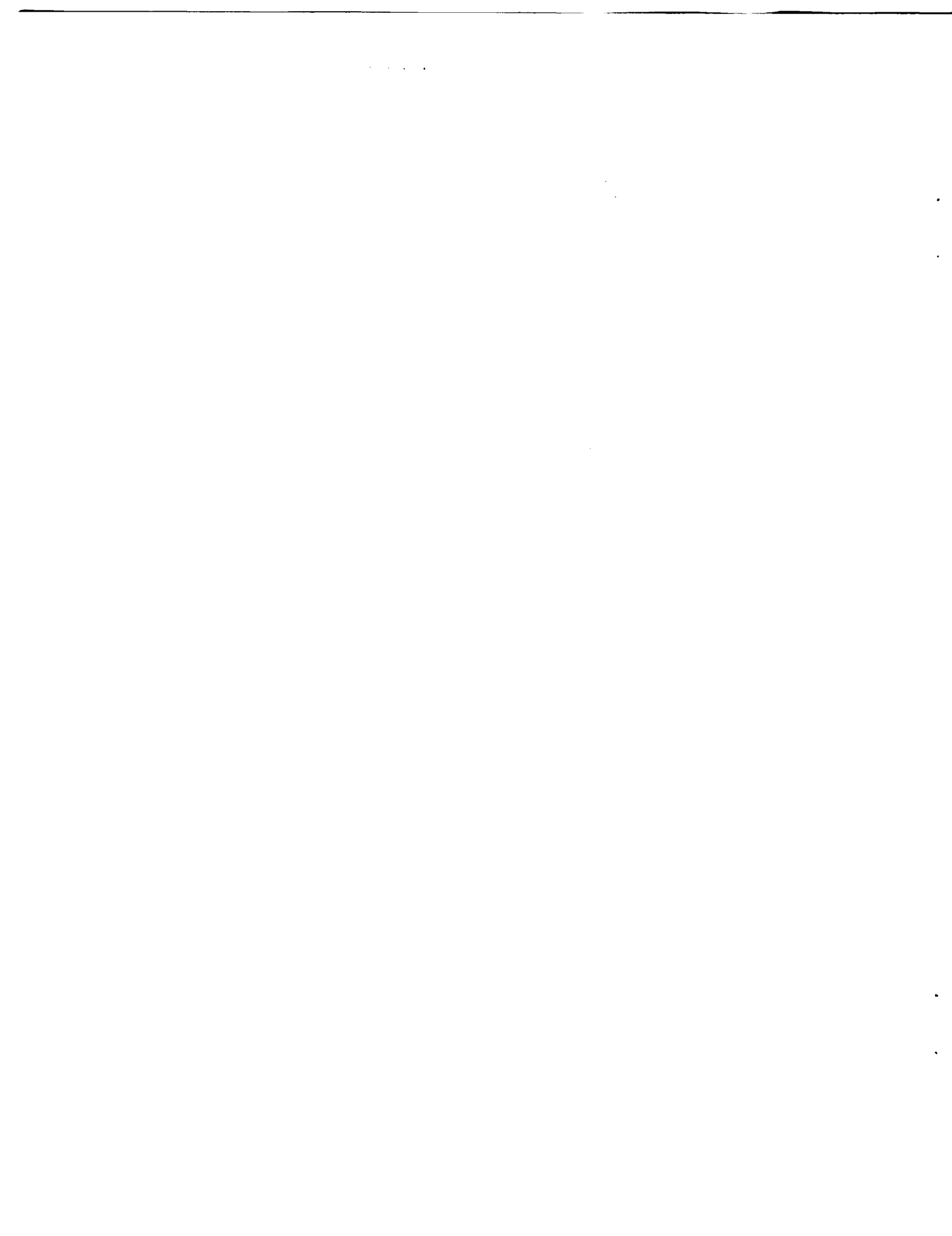
N95-12839

Unclas

G3/47 0027044

September 1994

National Aeronautics and
Space Administration
Langley Research Center
Hampton, Virginia 23681-0001



Abstract:

This report provides background data for the Boreal Ecosystem Atmosphere Study (BOREAS) sites, including daily, seasonal, interannual, and spatial variability of shortwave (SW) radiation at the Earth's surface. This background data, from Version 1.1 SW data set, was provided by the Surface Radiation Budget (SRB) Climatology Project established by the World Climate Research Program (WCRP).

Introduction:

The Boreal Ecosystem Atmosphere Study (BOREAS) experiment is an international scientific investigation of the interactions between the boreal forest biome and the atmosphere. While studying the interaction between the boreal forest biome and the physical climate system, the carbon cycle and biogeochemistry of the biome, and its ecological functioning, the BOREAS project will focus on the fate of the biome as a consequence of global change. Detailed measurements of radiation budget, sensible heat, water vapor, CO₂, momentum, surface state variables, meteorological variables, and key hydrological variables are planned, covering a 2-year period which began in 1993 (BOREAS Science Steering Committee, 1990; and Hall et al., 1993). These intense measurements encompass two study areas near the northern and southern boundaries of the boreal forest region in central Canada.

Surface radiation budget (SRB) parameters have been globally estimated with satellite data since 1986 as part of the World Climate Research Program (WCRP) (Suttles and Ohring, 1986). A Version 1.1 shortwave (SW) data set for the period March 1985 through December 1988 has been completed using International Satellite Cloud Climatology Project (ISCCP) C1 data as primary input (Whitlock et al., 1993). The SRB data presented in this report are the Version 1.1 results. When SRB results are combined with other data, such as ISCCP and Earth Radiation Budget Experiment (ERBE), a combination of parameters is available which may be useful as background information. While it is recognized that satellite-derived values may not be precise, the seasonal, interannual, and spatial variabilities may be useful for model studies, comparison with new data, and experiment planning purposes. These available SW parameters include (1) surface irradiances (all-sky downward, clear-sky downward, all-sky downward cloud forcing, and all-sky net), (2) all-sky direct/diffuse ratio, (3) all-sky surface albedo, (4) column atmospheric absorbed irradiance, (5) top-of-atmosphere (TOA) net (all-sky and clear-sky), (6) daylight-average cloud fraction and cloud optical depth, (7) surface air and skin temperatures, (8) column precipitable water vapor, and (9) column ozone. Diurnal variations of cloud fraction and cloud optical depth are also available. These data are presented in this report for the specific areas of concentration in the BOREAS experiment.

Sites and Methodology:

Locations of the BOREAS study sites relative to the ISCCP/SRB cells and the nearest Swiss Federal Institute of Technology Global Energy Budget Archive (GEBA) ground truth site are presented in Figure 1. The satellite data and experiment measurement areas have different spatial scales. The Mesoscale Study Area is roughly 1000 km by 1000 km covering a large portion of Saskatchewan and Manitoba, Canada. The Northern Study Area, approximately 20 km by 30 km, is located between Thompson and Nelson House, Manitoba. The Southern Study Area, 50 km by 120 km, is in the Prince Albert National Park (BOREAS Science Steering Committee, 1990; and Hall et al., 1993). The SRB cells for which satellite estimates are available in the Version 1.1 SRB product are 280 km by 280 km.

Maps suggest that vegetation and topography are uniform enough in this region that the monthly average of a single station within a cell is equal to the monthly average of a cell. It is also assumed that cell 5977 satellite results are comparable with monthly average measurements from The Pas ground truth site and that cell 6059 satellite results are representative of the BOREAS Northern Study Area. The results from cells 5975 and 5976 are averaged with 25% and 75% weighting factors to estimate values for the Southern Study Area. For the Mesoscale Study Area, all eight cells are linearly averaged to obtain estimated values. While it is recognized that complex interpolating methods could also have been used to estimate values in both the Southern and Mesoscale Study Areas, they are not incorporated in this study in order to preserve the fidelity of the original satellite estimates.

Accuracy of Satellite Estimates:

Downward SW irradiances are the only parameters that can be verified with long-term ground truth. Figure 2 indicates that the Pinker and Staylor satellite SRB algorithms track both each other and ground truth values from The Pas very closely. (Ground truth values are not presently available from the GEBA for 1988.) Both satellite algorithms detect the year-to-year variability during the summer period observed by ground truth measurements.

The SRB algorithms are physical radiative transfer models, not regression models. The Pinker algorithm uses an iterative procedure based on tables from delta-Eddington radiative transfer calculations (Pinker and Laszlo, 1992), while the Staylor method uses a highly parameterized, single-calculation radiative transfer model that has been tuned with experimental data from the early 1980's (Darnell et al., 1992). Each algorithm approaches the problem differently and uses a different combination of ISCCP

parameters as input to the calculations. Both algorithms have satisfied the Intercomparison of Radiation Codes in Climate Models (ICRCCM) model-validation tests.

Compared to The Pas ground truth data, both the Pinker (Figure 3) and the Staylor (Figure 4) algorithm results have biases within 1% of full-scale surface measurements and a total RMS (including bias) within 5%. The Version 1.1 SRB satellite results are not expected to be this accurate for all regions of the globe. If Pinker and Staylor values are averaged together and compared with ground truth from The Pas, the bias is -3 W m^{-2} and total RMS is 9 W m^{-2} .

Figure 5 compares surface albedo from both the Pinker and Staylor methods. Both satellite methods give similar surface albedo values unless there is winter snow present. The Staylor satellite values are derived from broadband ERBE satellite data, while the Pinker surface albedos are derived from ISCCP data to which narrowband to broadband transformations and the ERBE angular corrections were applied. Unfortunately, there are no large-scale surface albedo measurements available from The Pas, however, comparisons with data from other locations suggest that the Staylor albedo is most accurate over clear snow.

In both algorithms, the net SW is given by: $SW_{net} = SW_{down} \times (1 - \text{albedo}_{surface})$. Therefore, the accuracy of surface albedo directly affects the calculation of surface SW net irradiances from surface SW downward values for both satellite algorithms. Figure 6 shows that the surface net SW differences between the Pinker and Staylor algorithms are quite moderate for this particular region. Relative to the maximum SW net value, bias is 3% and total RMS is 5%. The large differences in surface albedo over snow are offset by low values in downward irradiances in the winter months. Surface albedo has a secondary atmospheric backscattering effect on the calculation of surface downward SW values. Pinker albedo uncertainty over snow may partially explain why that algorithm's estimate for downward irradiance has slightly larger errors than the Staylor method (see Figures 3 and 4). Both satellite algorithms appear to produce reasonable estimates of downward and net SW irradiance.

Satellite SRB Values:

Many of the satellite SRB values are presented for either the Northern, Southern, or Mesoscale Study Areas. As mentioned previously, the satellite values for the Southern Study Area are weighted averages and the satellite values for the Mesoscale Study Area are linear averages. These averages are calculated when at least half of the smaller regions have data. Therefore, at least one of the two Southern

values must be available to calculate an average; similarly, four or more Mesoscale values are required. Data gaps caused by insufficient satellite values occur most frequently, but not exclusively, during the winter months of December 1986, 1987, and 1988.

Figures 7, 8, and 9 compare Pinker and Staylor downward SW irradiance for the three study areas. Downward SW irradiance is quite seasonal with the greatest interannual variability occurring in the summer months. Figures 10 and 11 show Pinker-derived diurnal variation for both the Northern and Southern Study Areas. The results represent the average of 4 years of Pinker algorithm results for the same hour and month. (The Staylor results are not calculated on a 3-hourly basis.) Exceptions are the months of January and February where only 3 years of data are available from the SRB data set. However, no average is calculated for December in the Northern Study Area because at least two of the four values for December must exist in order to average the data. The apparent inconsistencies between adjacent months are caused by changes in the diurnal characteristics of clouds.

The effects of cloudy conditions on downward SW irradiance are shown in Figures 12, 13, and 14. This "cloud forcing" parameter is the difference between monthly average clear-sky and all-sky values. This parameter represents the loss of flux at the surface due to clouds in the atmospheric column. Cloud forcing is dominated by cloud transmission effects, but are also influenced by aerosol and water vapor changes. Cloud forcing from the Pinker and Staylor algorithms usually compares to within 10 W m^{-2} . Again, most interannual variability occurs during the summer months. The Staylor algorithm always produces a more negative cloud forcing in the snow-covered winter months. It should be noted that neither SRB algorithm uses ISCCP cloud optical depth. The Pinker algorithm uses a modified form of the Stephens et al. (1984) parameterization while the Staylor algorithm applies a relative-threshold technique for cloud transmittance (Darnell et al., 1988).

Figures 15, 16, and 17 present surface net SW irradiance. The Pinker and Staylor results compare closely. The Pinker snow-albedo uncertainty does not cause a large deviation because of the low downward irradiance in winter. Figures 18, 19, and 20 show satellite estimates of surface SW albedo for the three study areas. Both algorithms produce similar values for the warmer months; however the snow values differ dramatically.

The downward SW direct/diffuse ratio from the Pinker algorithm for the three study areas is presented in Figure 21. The accuracy of the ratio of direct solar flux to diffuse skylight is uncertain because ground truth data from U.S. sites are limited. Satellite SRB ratios are approximately 25% lower than those from Omaha, Nebraska; for other sites, the satellite data are as low as 20% of ground-site values. The

accuracy of the ground truth methods, as well as the accuracy of the satellite algorithm, remains undetermined for this parameter.

Figure 22 gives the Pinker algorithm estimate of the amount of irradiance absorbed within the atmosphere. This parameter, Pinker SW atmosphere absorbed, is obtained by subtracting the Pinker top-of-atmosphere (TOA) net SW irradiance from the surface net SW irradiance. These values are primarily a function of ISCCP-estimated precipitable water vapor with some contribution from the ISCCP estimated ozone, seasonal solar zenith angle, and aerosol type.

Supporting Data:

Daytime-average cloud fraction and cloud optical depth from ISCCP are presented in Figures 23 and 24. All three areas usually have a similar range of monthly average cloud fraction (0.5 to 0.8) and cloud optical depth (4 to 15) except in the late fall and winter periods. ISCCP cloud fraction and cloud optical depth are not considered reliable during winter months over snow because of the satellite bands selected for use in the C1 version data processing (Rossow et al., 1991). The new ISCCP D1 data set should eliminate this problem over bright surfaces. Figures 25 through 28 show diurnal variation of cloud fraction and cloud optical depth from ISCCP data for both the Northern and Southern Study Areas. The results are based on a 4-year average for each data month, except for January and February where only 3 years of SRB data are available. A strong seasonal pattern is not evident over vegetated surfaces.

Figures 29 and 30 present ISCCP-derived surface temperatures. Figure 29 shows air temperature as obtained from the Tiros Operation Vertical Sounder (TOVS) data, and Figure 30 presents ISCCP-estimated skin temperature. As expected, there is a strong seasonal pattern with a 5° K to 10° K difference between the Northern and Southern Study Areas. ISCCP-derived precipitable water and ozone, as obtained from the TOVS instrument, are presented in Figures 31 and 32. There is little regional variation for these two parameters, but seasonal variations are strong. The appearance of a steady increase in the magnitude of the seasonal observation for precipitable water (Figure 31) may be real or could be the result of a problem in the reduction of the NOAA-9 TOVS data. There is also significant variability in ISCCP-derived ozone on a year-to-year basis.

Figures 33 and 34 show ERBE satellite TOA net SW flux histories. The all-sky values in Figure 33 show systematic agreement for the three study areas. The Southern Study Area values are a few $W m^{-2}$ lower than the Northern Study Area. The clear-sky values in Figure 34 tend to agree for all three study areas except during March 1985 and 1986. Surface albedo values from Figures 18, 19, and 20 suggest a

north-to-south snow-melt gradient as the cause of the spread in clear-sky TOA net irradiance for these 2 months.

Monthly Interannual and Spatial Variability:

Cosine curves were fitted to time histories of all-sky downward, cloud forcing, and net irradiances in order to examine interannual and spatial variability of surface radiation parameters. In this analysis, the Pinker and Staylor results have been averaged to produce a single estimate prior to curve-fitting. Figures 35 and 36 show all-sky downward results for the Northern and Southern Study Areas, respectively. Most interannual variability in downward SW flux occurs during the summer months. The amplitude of the seasonal curve is slightly larger for the Southern Study Area. The standard deviation is about 11 W m^{-2} for interannual variability of all-sky downward irradiance.

Figures 37 and 38 present cloud forcing results. Magnitudes of cloud forcing are nearly identical for both study areas, however, summer-season variabilities may occur in only one region in a given year. The standard deviation for interannual variability of cloud forcing is approximately 10 W m^{-2} . Figures 39 and 40 give monthly average clear-sky downward irradiance values for the Northern and Southern Study Areas, respectively. These results were obtained by subtracting the cloud forcing (Figures 37 and 38) from the all-sky downward SW (Figures 35 and 36) to obtain clear-sky downward SW for each region. As expected, clear-sky values are slightly larger for the Southern Study Area. Standard deviation of interannual variability is approximately 6 W m^{-2} for clear-sky downward irradiance.

Figures 41 and 42 show that the surface net SW fluxes for the two study regions are within 7 to 10 W m^{-2} of each other, with greatest interannual variability occurring during the summer. Standard deviation is approximately 14 W m^{-2} for interannual variability of all-sky net irradiance. Figures 43 and 44 present Northern and Southern Study Area seasonal results, respectively, for downward SW and net SW. These data show that both monthly average SW downward and net SW irradiances are 5 to 7 W m^{-2} higher in the Southern Study Area than in the Northern Area over most of the year.

Daily Variability:

The comparison of clear-sky, all-sky, and TOA monthly downward SW flux with daily all-sky downward SW irradiances is presented in Figures 45 and 46. The TOA flux does not include atmospheric effects, while the clear-sky model considers atmospheric effects but does not have cloud effects. The all-

sky results account for both atmospheric and cloud effects. There are instances when either Pinker or Staylor predictions for all-sky downward SW irradiance are greater than the clear-sky monthly model. This is due largely to low aerosol values. Clearly, the all-sky monthly results are based on an average of the daily all-sky downward SW values. The Pinker and Staylor data are fairly evenly distributed about the all-sky monthly curve. Both the Northern and Southern Study Areas may have days during the summer which have very low SW irradiances, approaching winter values.

Conclusions:

Version 1.1 WCRP/SRB satellite estimates of surface downward SW all-sky irradiance tracked ground truth measurements closely and detected the same year-to-year variabilities. Statistical correlation between the satellite estimates and ground truth in the BOREAS region indicates a bias of -3 W m^{-2} , and total RMS (including bias) is 9 W m^{-2} . The satellite estimates show a strong seasonal variability in both all-sky SW downward and net SW surface irradiance as would be expected from solar geometry effects. Time histories of monthly average, all-sky values are more sinusoidal than many other regions of the globe, however. Fitted cosine curves suggest that all-sky spatial variability between the Northern and Southern Study Areas is only 5 to 7 W m^{-2} for both the downward and net SW parameters. The annual range of downward SW values is from 8 to 235 W m^{-2} .

Interannual variability of downward SW and net SW irradiance is small and seems to occur mostly during the summer months. The standard deviation of interannual variability is 11 and 14 W m^{-2} for downward and net SW irradiance, respectively. During summer months, interannual variability may approach three times the standard deviation, and significant variability may occur in only one of the study regions in a given year. Magnitudes of cloud forcing are seasonal and nearly identical for both study areas, however, summer-season variabilities may occur in only one of the study regions in a given year. Cloud forcing during the summer months is a major cause for interannual variability in the all-sky downward SW irradiance.

Daily variability of all-sky downward SW flux can be quite large. During the summer months, the daily all-sky downward SW irradiances range from 80 to 347 W m^{-2} for the Northern Study Area and from 27 to 362 W m^{-2} for the Southern Study Area. The variability is largest during the summer months when all-sky daily SW irradiances often exceed clear-sky monthly-average predictions and cloud forcing is the largest.

Estimates of clear-sky downward SW irradiance for the Northern Study Area range from 20 to 335

$W m^{-2}$ on a seasonal basis with an interannual standard deviation of $6 W m^{-2}$. Southern Study Area values appear to be 8 to $10 W m^{-2}$ higher than those of the northern region. Pinker and Staylor broadband surface albedos are in reasonable agreement over vegetated surfaces. Large differences occur in the estimation of broadband surface albedo over snow, however. This is not a serious problem in the BOREAS region because solar illumination is low when snow conditions exist. As a result, large differences in net SW surface irradiance between the Pinker and Staylor algorithms do not exist at any time of the year. ISCCP cloud fraction and cloud optical depth results suggest that monthly average cloud conditions are generally similar, but not always identical, for the Northern and Southern Study Areas over vegetated surfaces. Strong seasonal variations are not evident. Monthly average cloud fraction ranges between 0.5 and 0.8. Cloud optical depths usually range between 4 and 15. No conclusions were reached for the winter months because ISCCP cloud results are not considered reliable over snow.

NOAA-9 TOVS satellite results indicate a slowly increasing amplitude in the seasonal peak-to-trough oscillation of precipitable water. It is not known whether this interannual variability actually existed or whether it is the result of an error in the satellite measurements. ISCCP estimates of both surface air temperature and skin temperature show a 5° to 10° relative difference between the Northern and Southern Study Areas for both parameters. The Southern Study Area is the warmest. Absolute values of the satellite-derived precipitable water, air temperature, and skin temperature data have not been verified. The absolute accuracies of satellite-derived broadband surface SW albedo, downward SW direct/diffuse ratio, and surface temperatures are unknown at this time. The results from this study are based on observations from a 4-year period, the above conclusions may not prove accurate for longer periods of time.

References

BOREAS Science Steering Committee, 1990: Charting the Boreal Forest's Role in Global Change. *EOS*, 72, 33-40.

Darnell, W.L., W.F. Staylor, S.K. Gupta, and F.M. Denn, 1988: Estimation of Surface Insolation Using Sun-Synchronous Satellite Data. *J. Climate*, 1, 820-835.

Darnell, W.L., W.F. Staylor, S.K. Gupta, N.A. Ritchey, and A.C. Wilber, 1992: Seasonal Variation of Surface Radiation Budget Derived from International Satellite Cloud Climatology Project C1 Data: *J. Geophys. Res.*, 97, 15741-15760.

Hall, F.G., P.J. Sellers, M. Apps, D. Baldocchi, J. Cihlar, B. Goddison, H. Margolis, and A. Nelson, 1993: BOREAS: Boreal Ecosystem-Atmosphere Study. IEEE Geoscience and Remote Sensing Society Newsletter, March 1993, 9-16.

Pinker, R. and I. Laszlo, 1992: Modeling Surface Solar Irradiance for Satellite Applications on a Global Scale. *J. Appl. Meteo.*, 31, 194-211.

Rossow, W.B., L.C. Garder, P.-J. Lu, and A. Walker, 1991: International Satellite Cloud Climatology Project (ISCCP) Documentation of Cloud Data. WMO/TD-No. 266, Revised March 1991, World Meteorological Organization, Geneva, 76 pp. plus 3 appendices.

Stephens, G.L., S. Ackerman, and E. Smith, 1984: A Shortwave Parameterization Revised to Improve Cloud Absorption. *J. Atmos. Sci.*, 41, 687-690.

Suttles, J.T. and G. Ohring, 1986: Surface Radiation Budget for Climate Applications. NASA RP 1169, 136 pp.

Whitlock, C.H., T.P. Charlock, W.F. Staylor, R.T. Pinker, I. Laszlo, R.C. DiPasquale, and N.A. Ritchey, 1993: WCRP Surface Radiation Budget Shortwave Data Product Description - Version 1.1. NASA TM 107747, 28 pp.

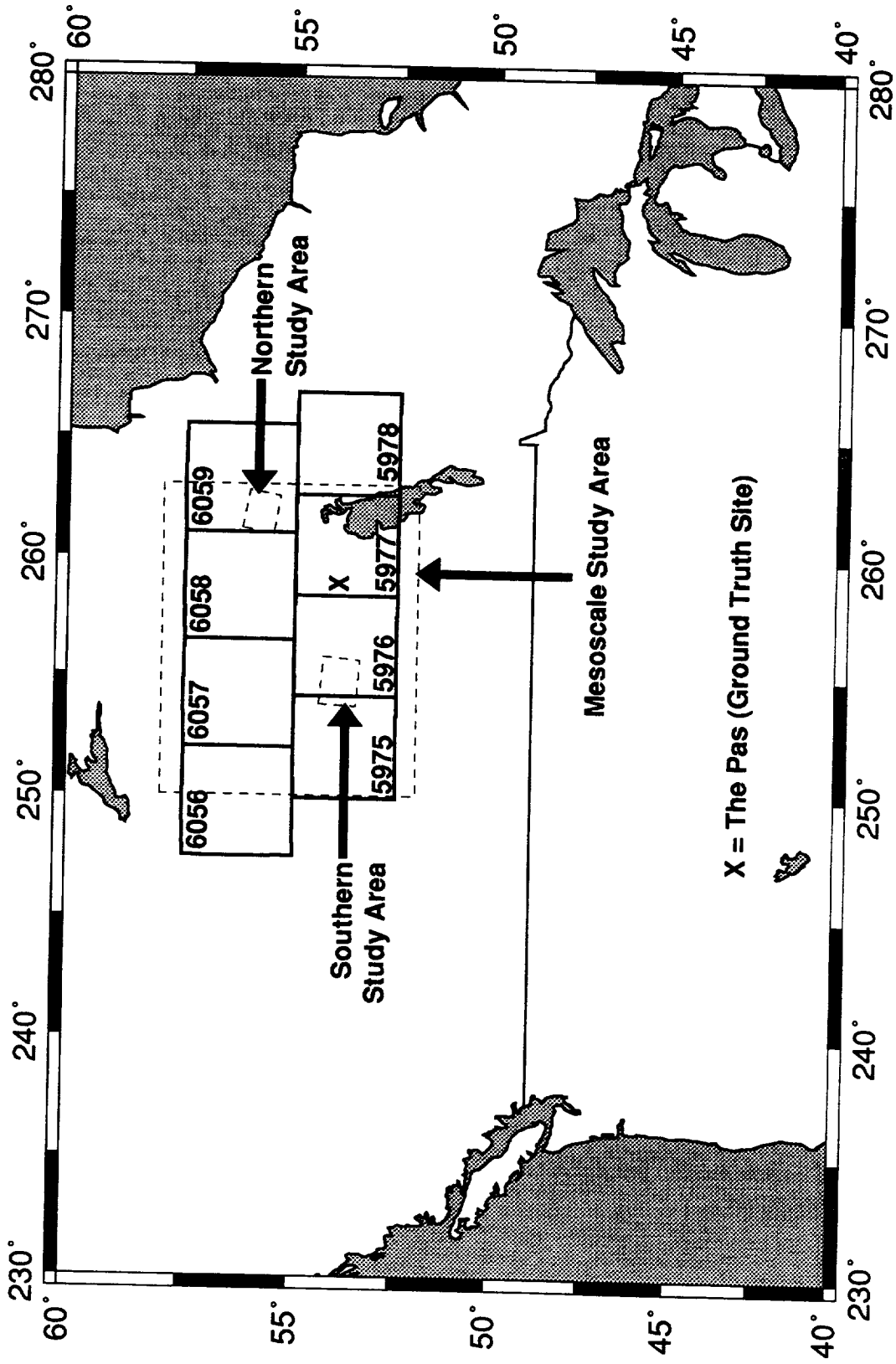


Figure 1. Location of study sites relative to ISCCP/SRB cell numbers.

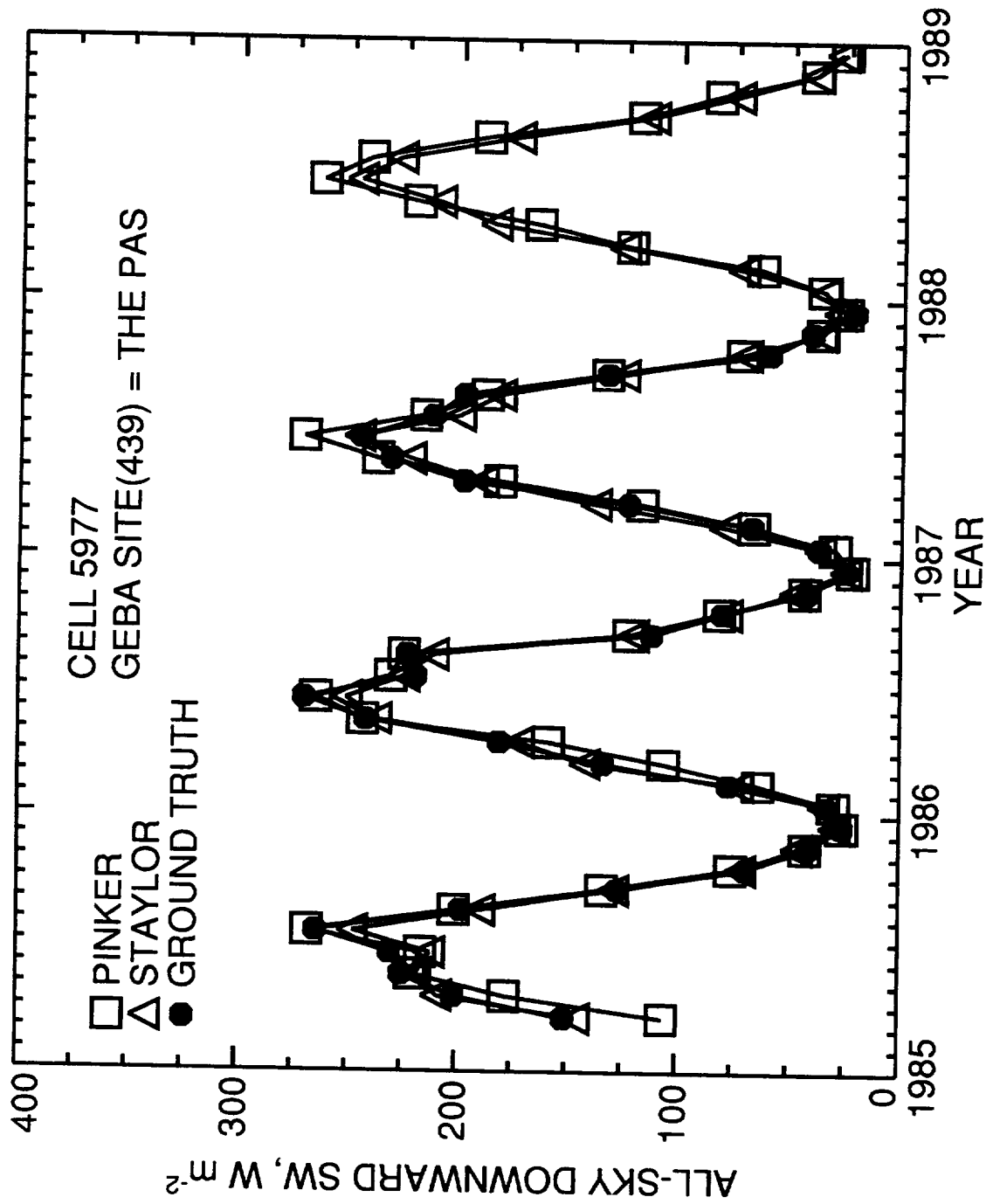


Figure 2. Comparison of surface downward SW all-sky flux for The Pas from 1985 to 1989.

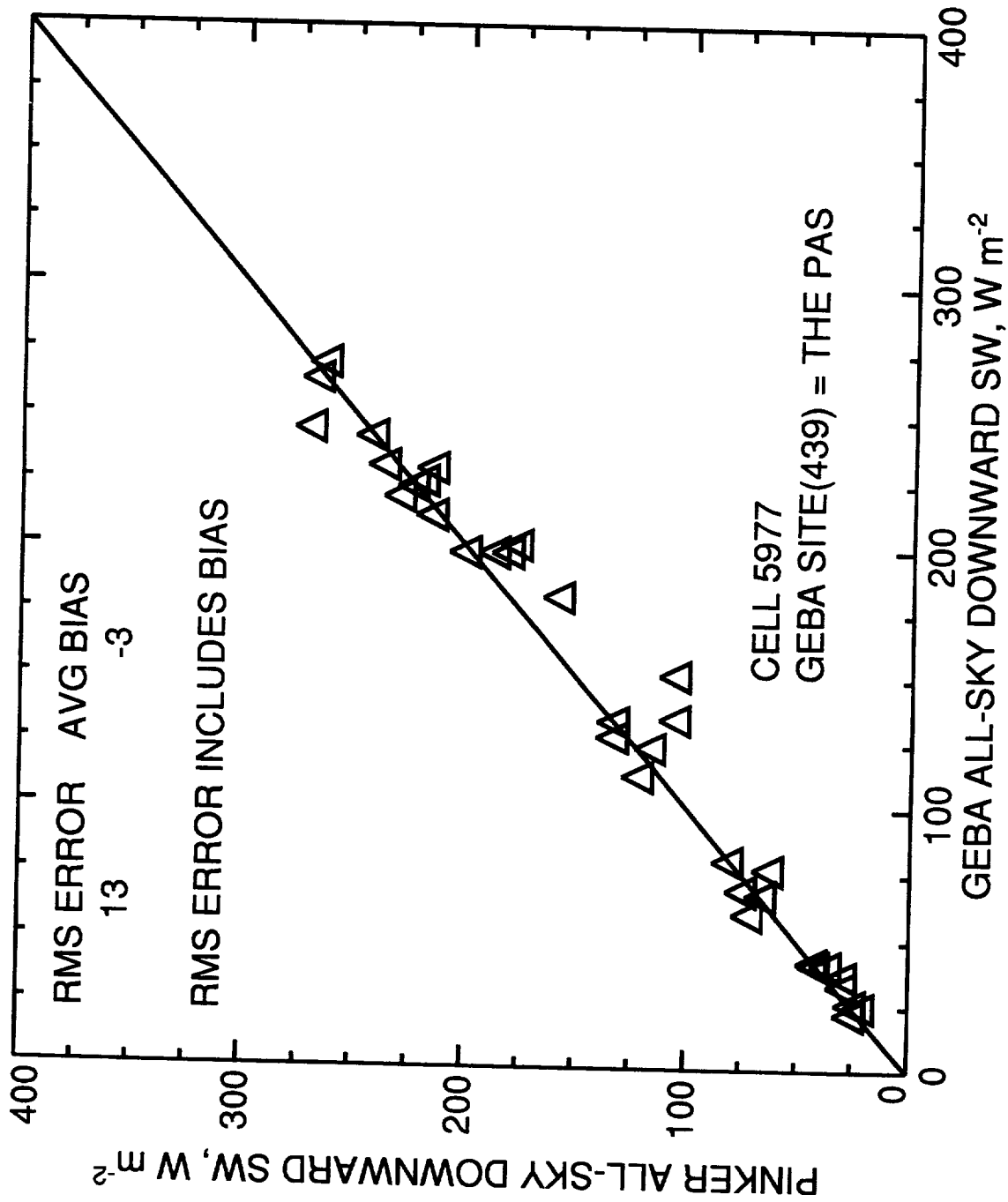


Figure 3. Pinker-to-ground truth comparison of surface downward SW all-sky flux for The Pas from 1985 to 1989.

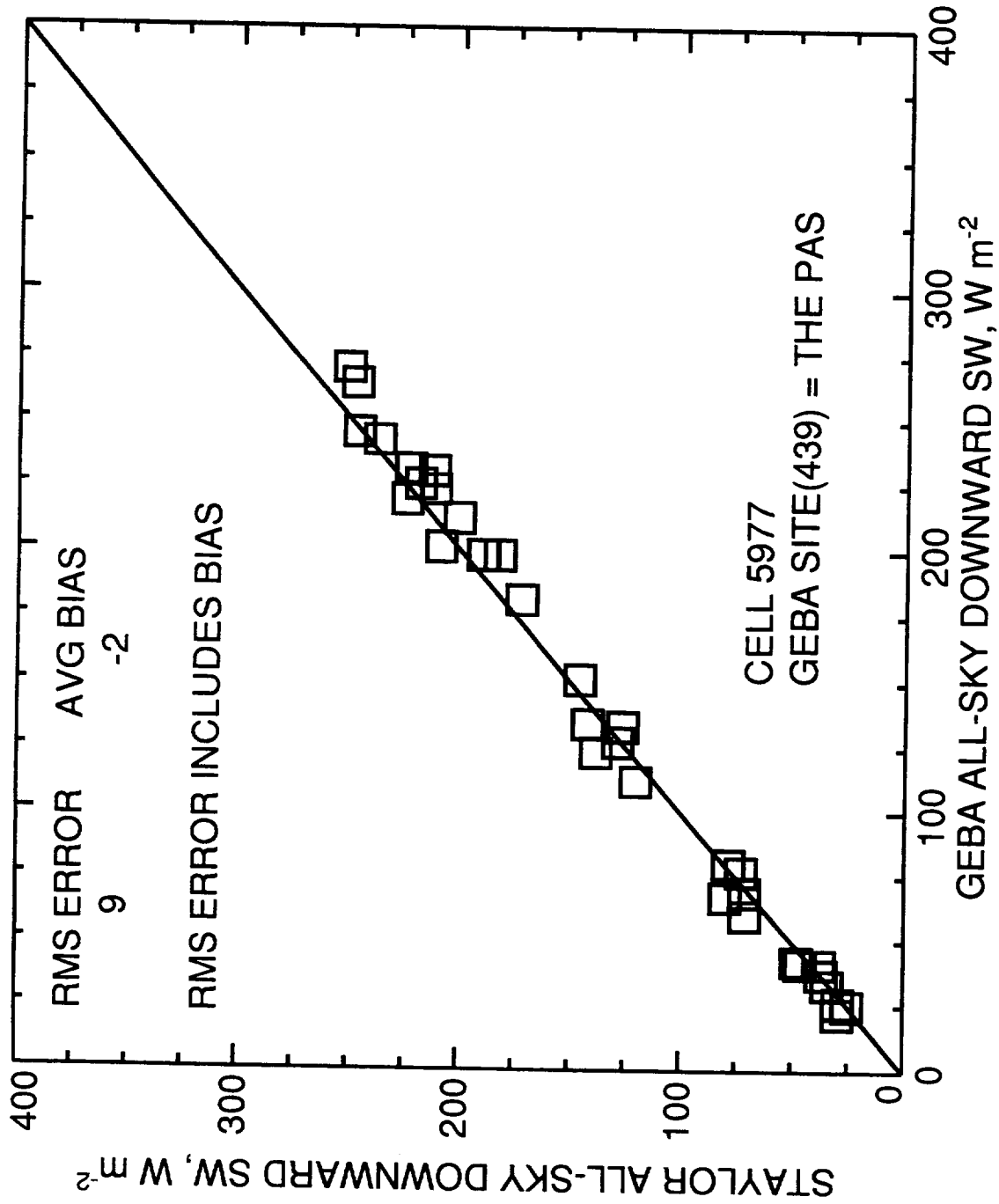


Figure 4. Staylor-to-ground truth comparison of surface downward SW all-sky flux for The Pas from 1985 to 1989.

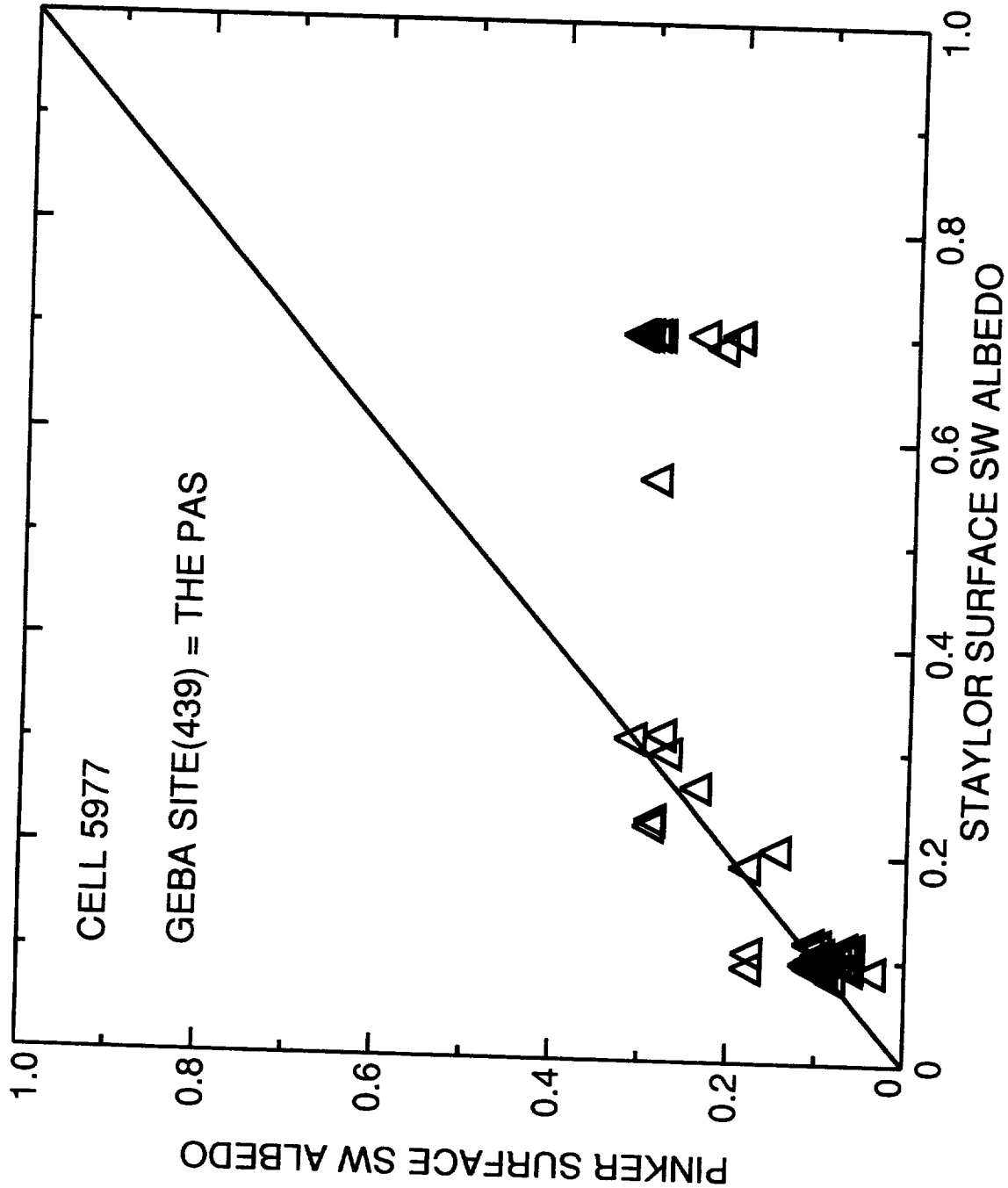


Figure 5. Comparison of Pinker and Staylor surface SW albedo for The Pas from 1985 to 1989.

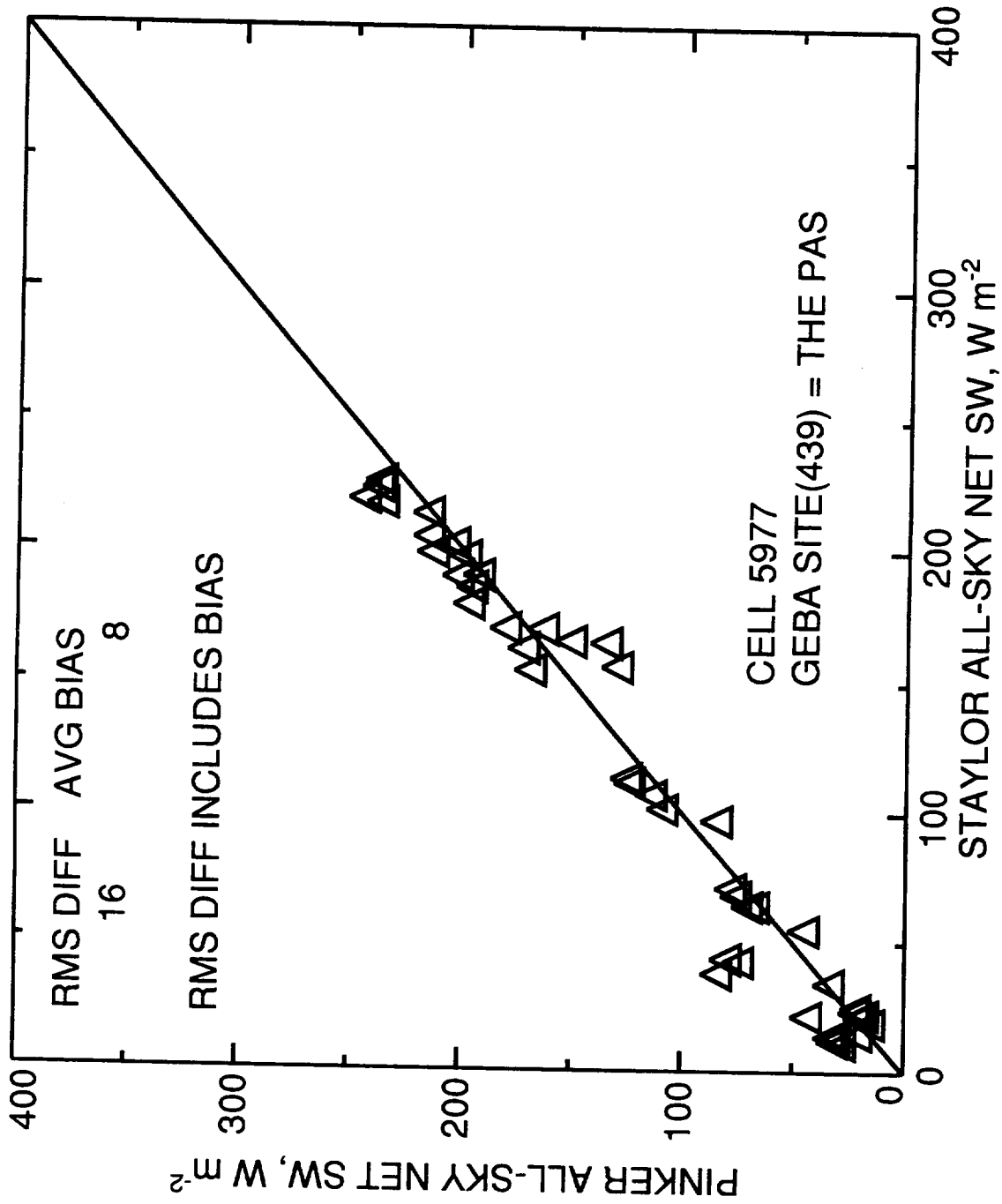


Figure 6. Comparison of Pinker and Staylor surface all-sky SW net flux for The Pas from 1985 to 1989.

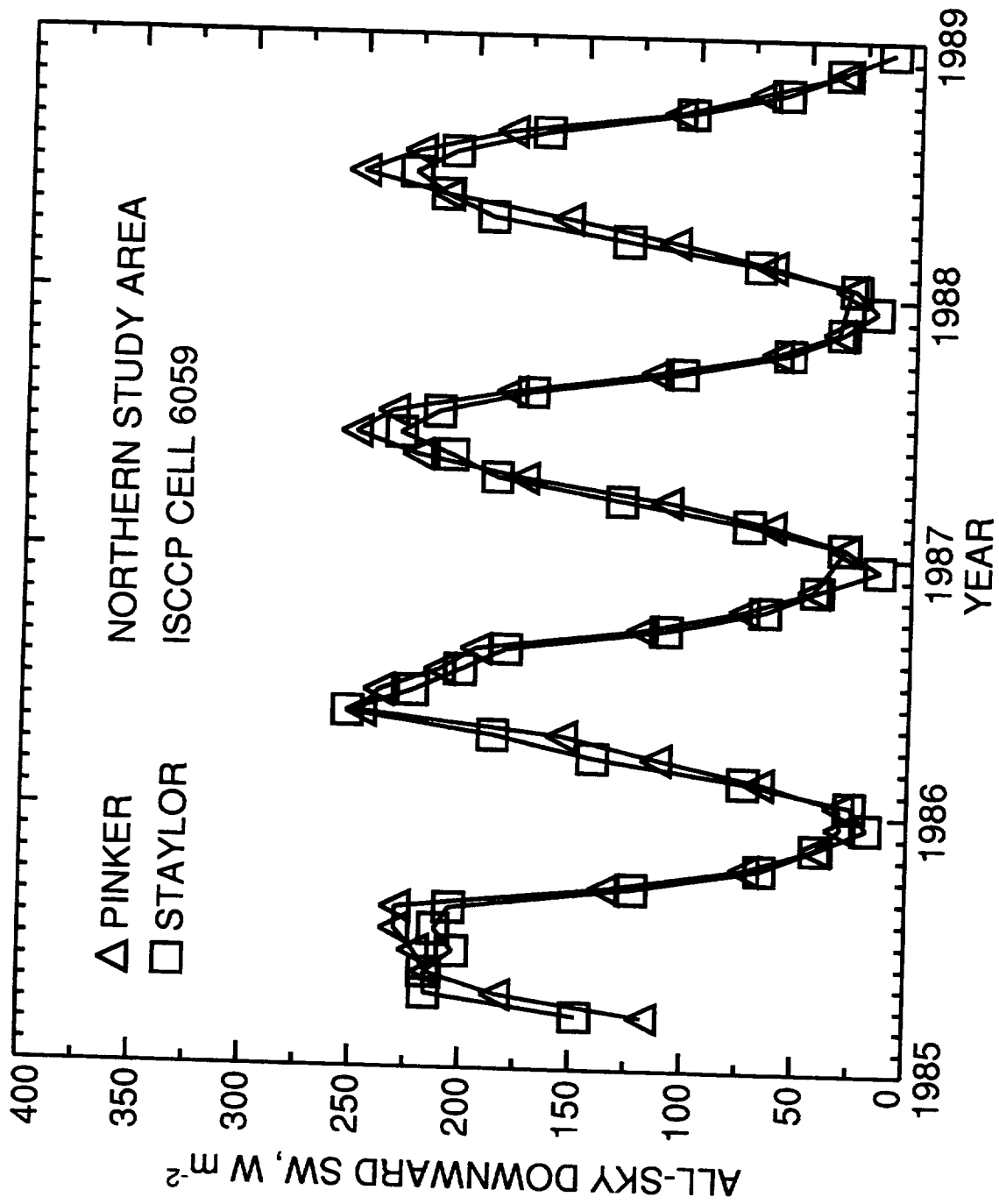


Figure 7. Surface all-sky downward SW flux for the Northern Study Area.

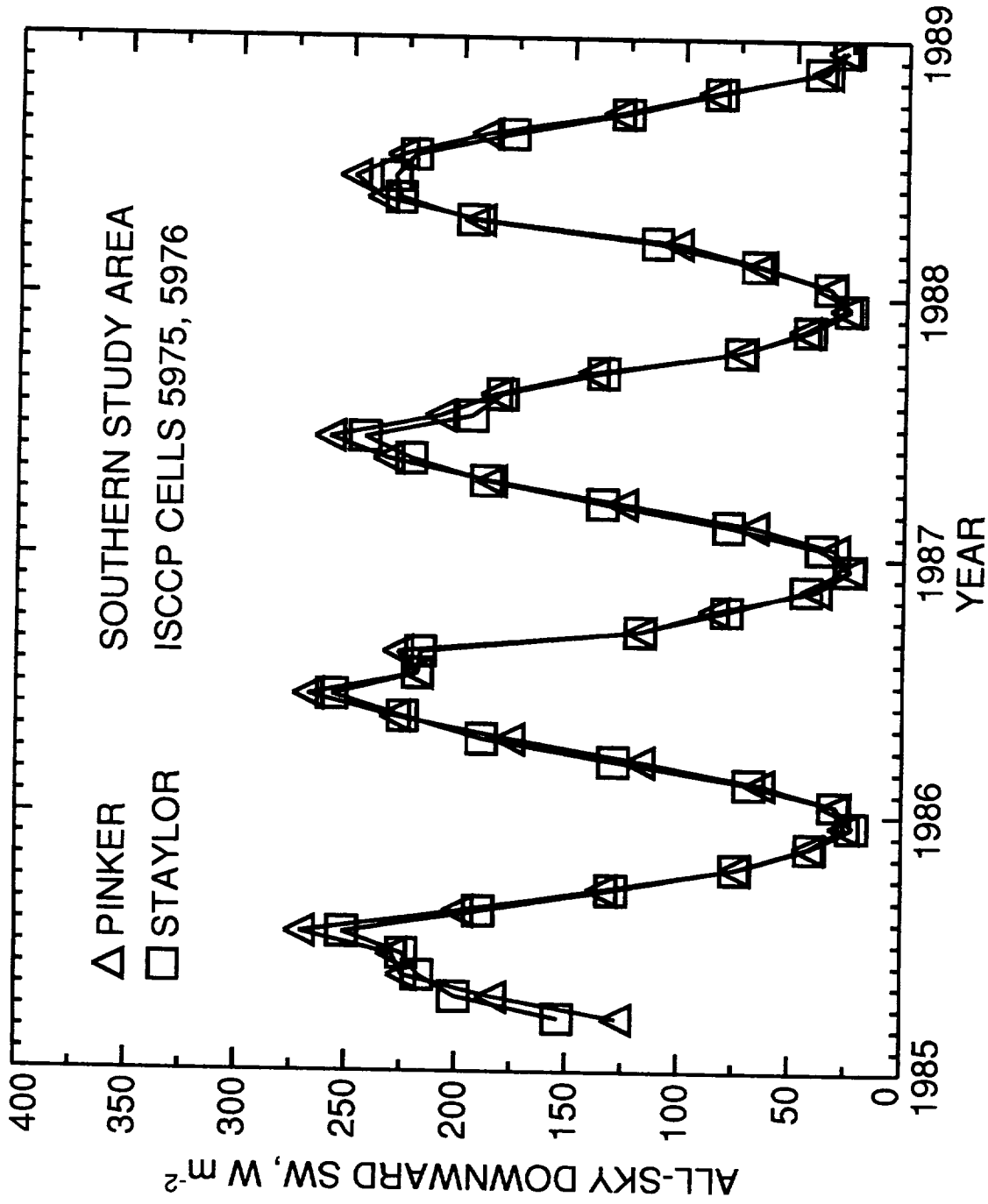


Figure 8. Surface all-sky downward SW flux for the Southern Study Area.

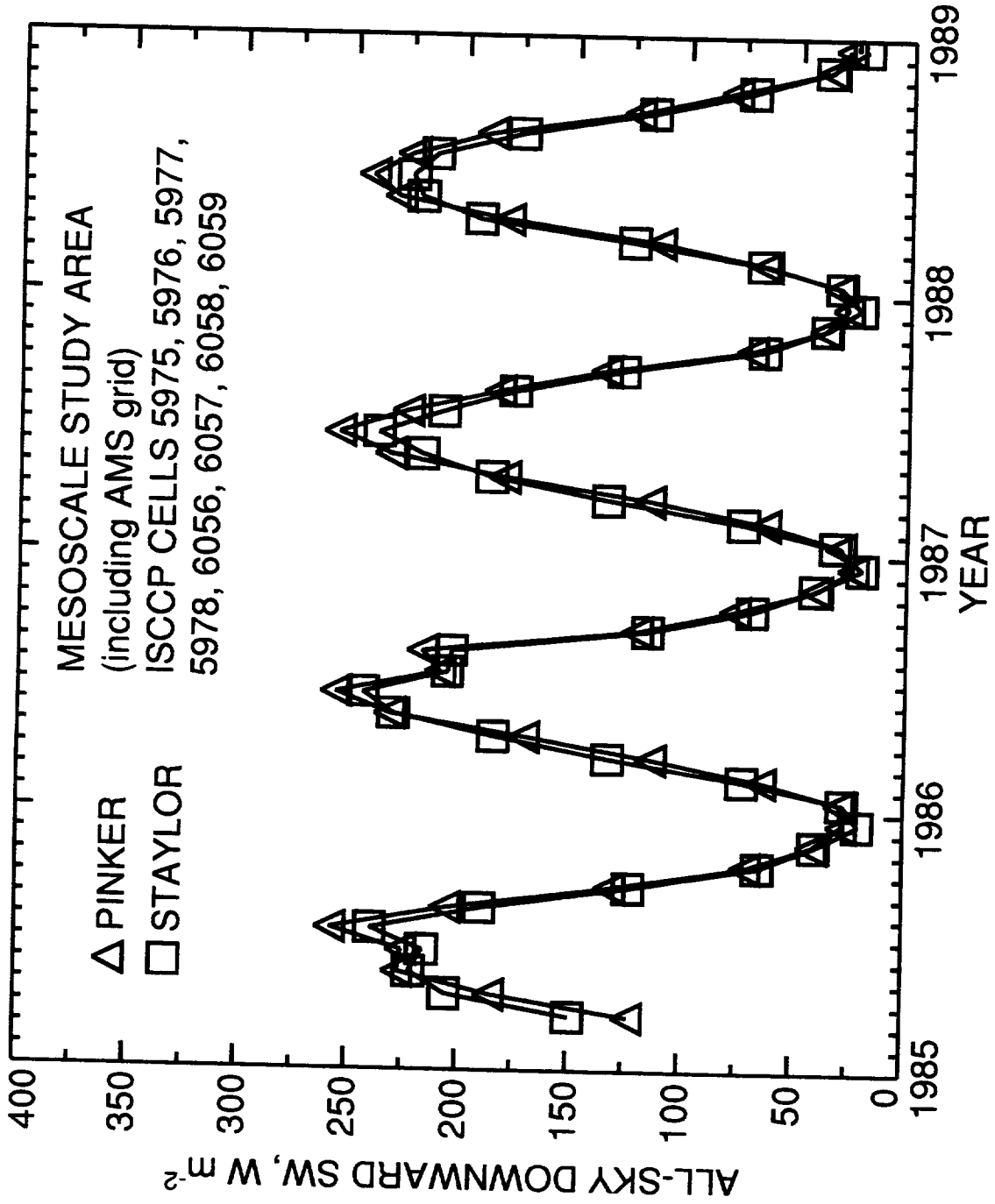


Figure 9. Surface all-sky downward SW flux for the Mesoscale Study Area.

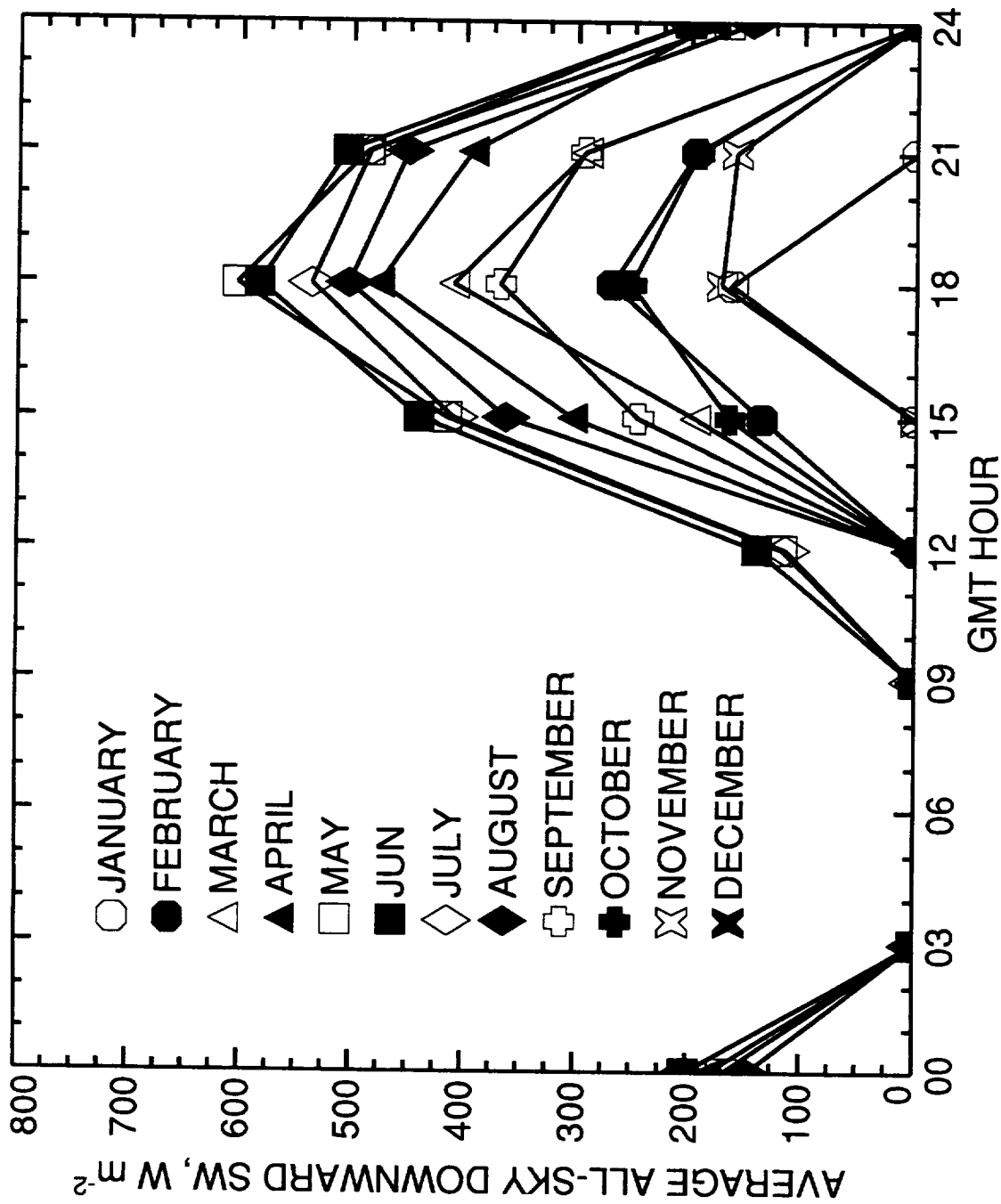


Figure 10. Average Pinker-derived surface all-sky downward SW flux by month for Northern Study Area.

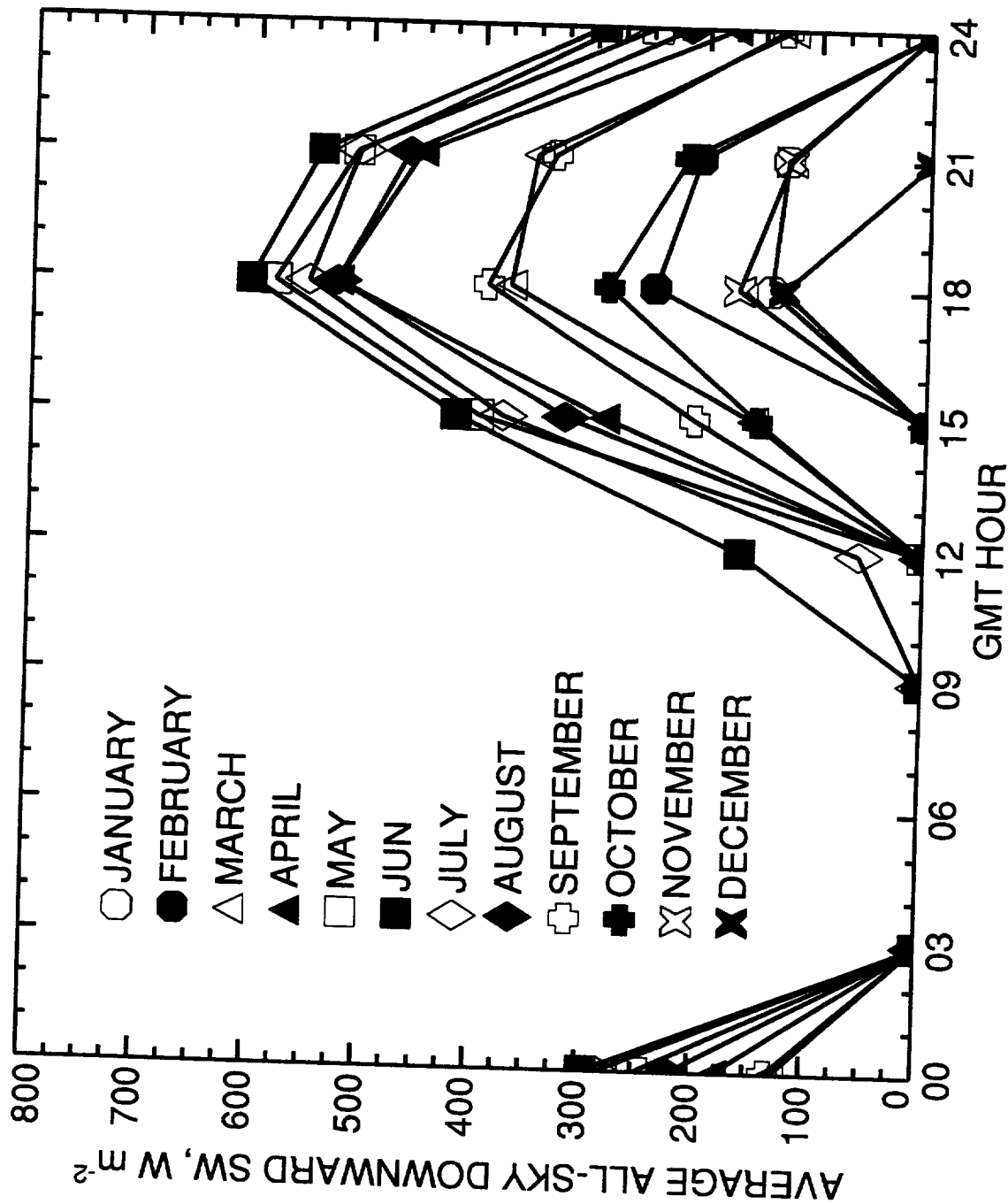


Figure 11. Average Pinker-derived surface all-sky downward SW flux by month for Southern Study Area.

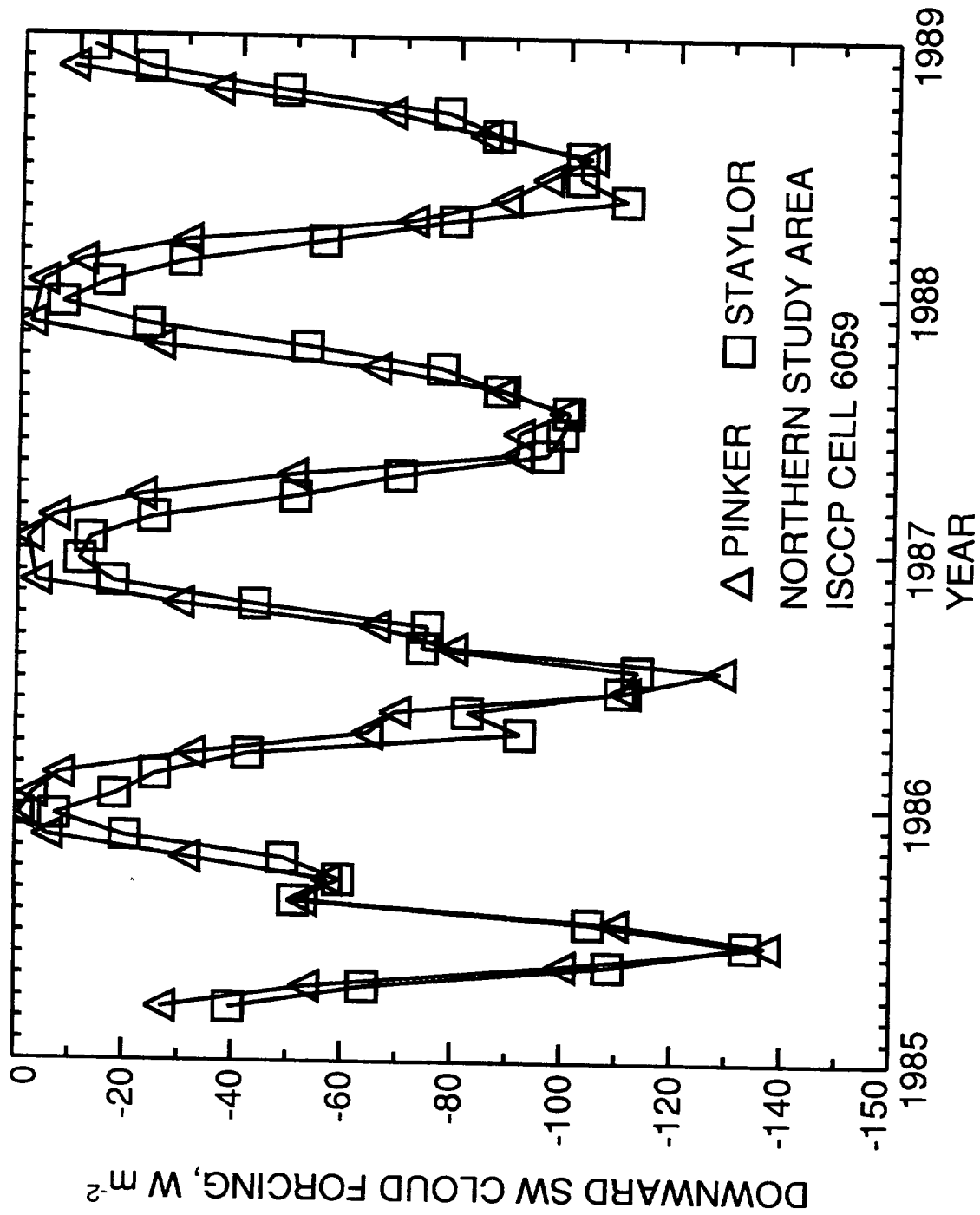


Figure 12. Surface downward SW cloud forcing over the Northern Study Area.

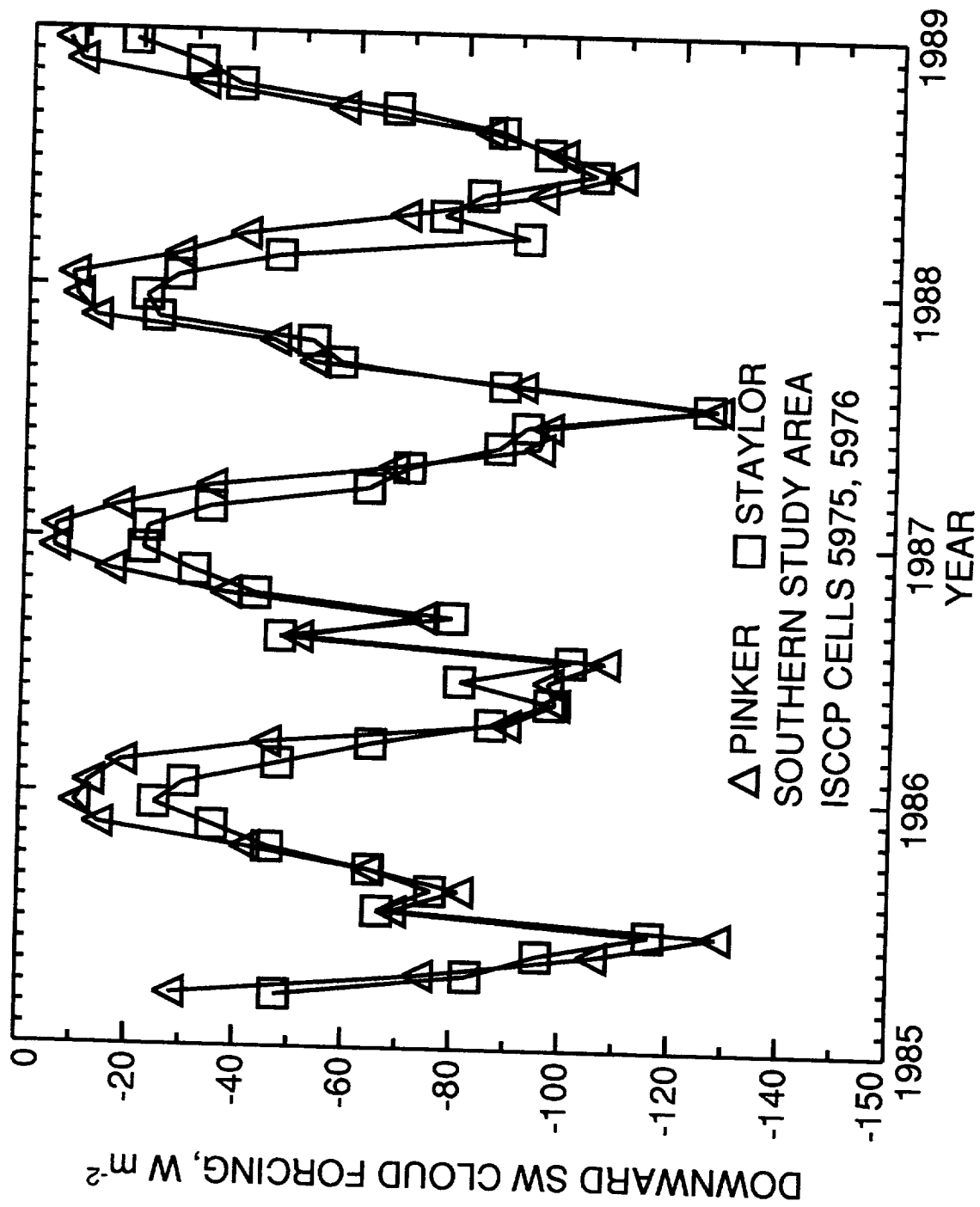


Figure 13. Surface downward SW cloud forcing over the Southern Study Area.

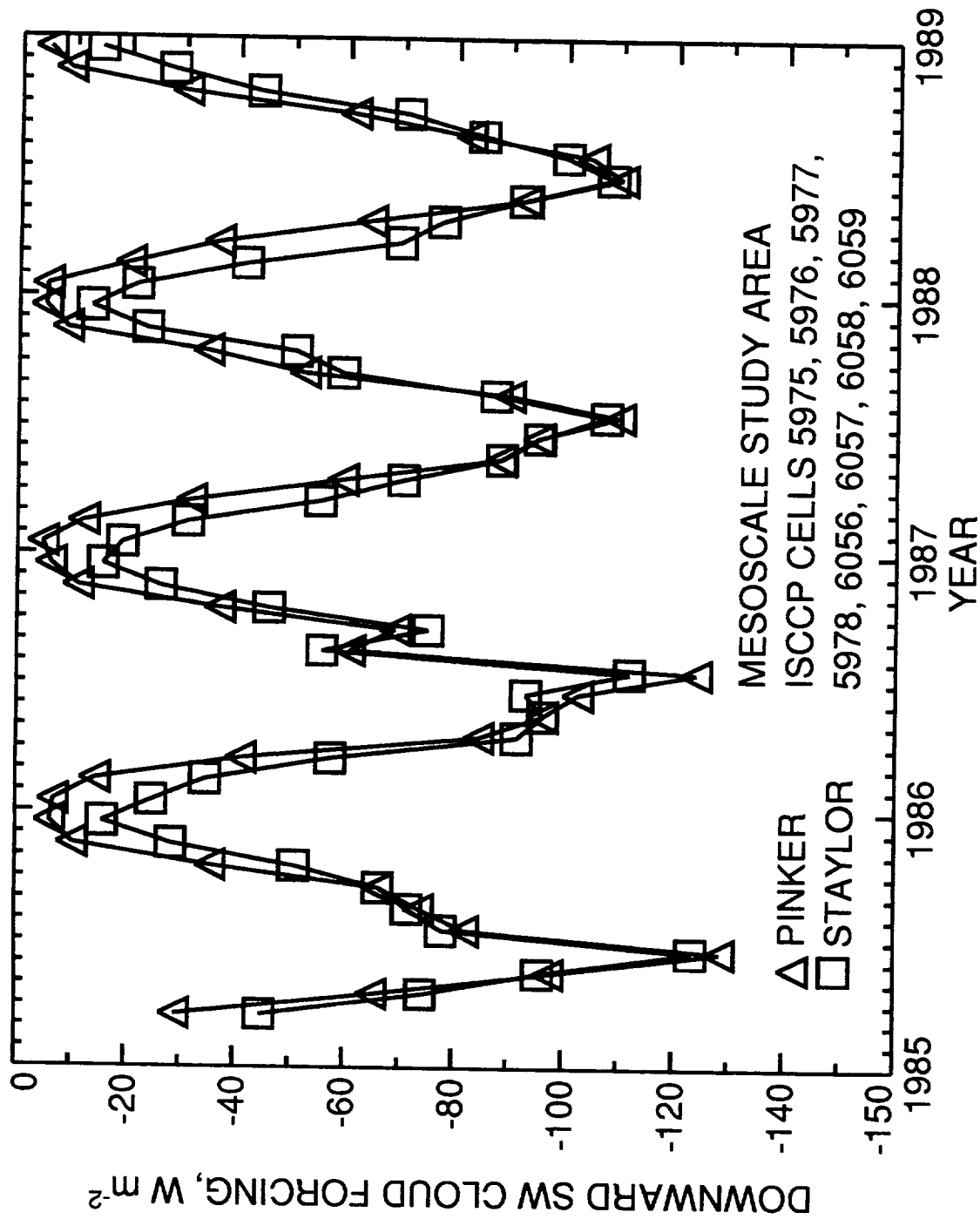


Figure 14. Surface downward SW cloud forcing over the Mesoscale Study Area.

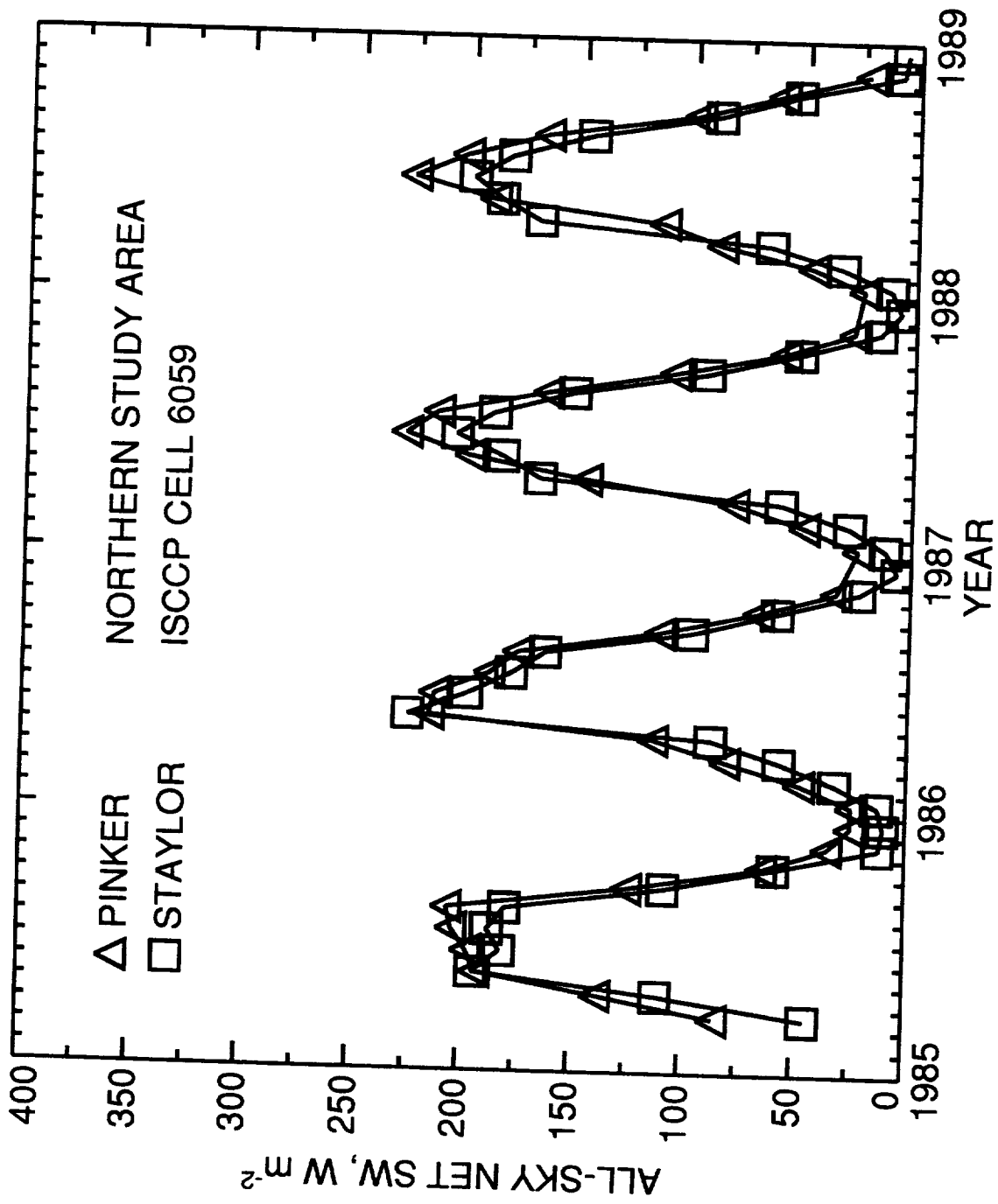


Figure 15. Surface all-sky net SW flux over the Northern Study Area.

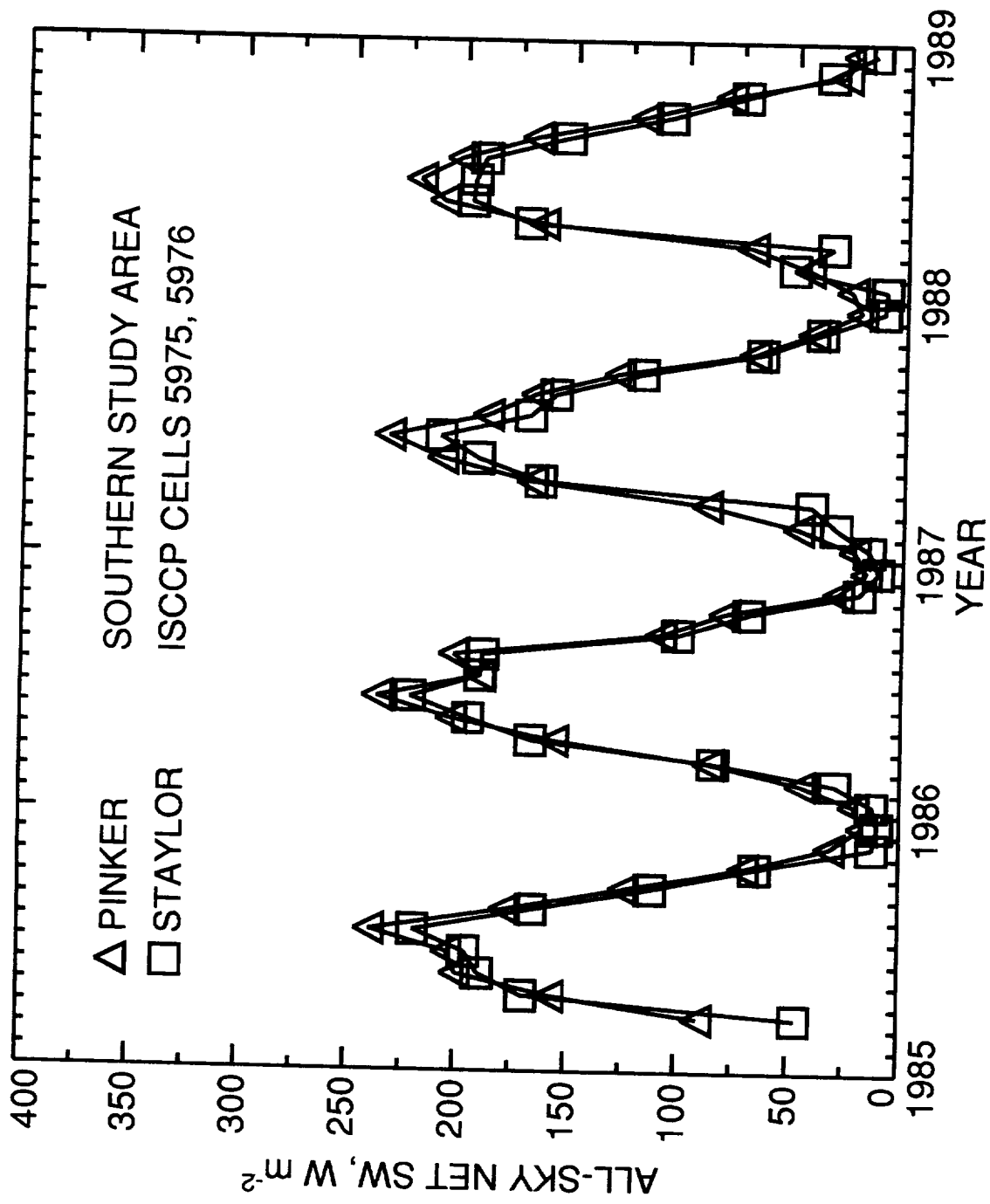


Figure 16. Surface all-sky net SW flux over the Southern Study Area.

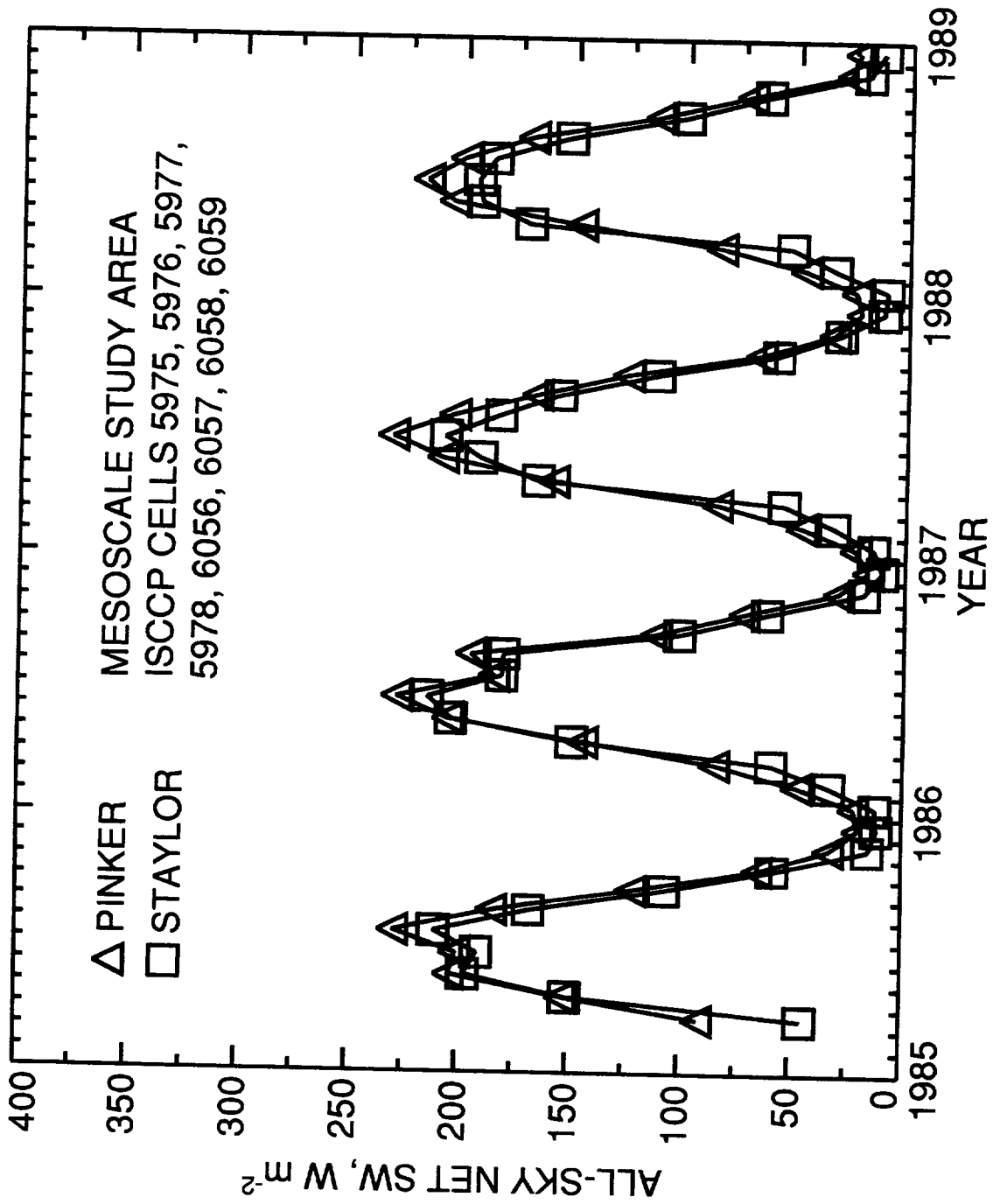


Figure 17. Surface all-sky net SW flux over the Mesoscale Study Area.

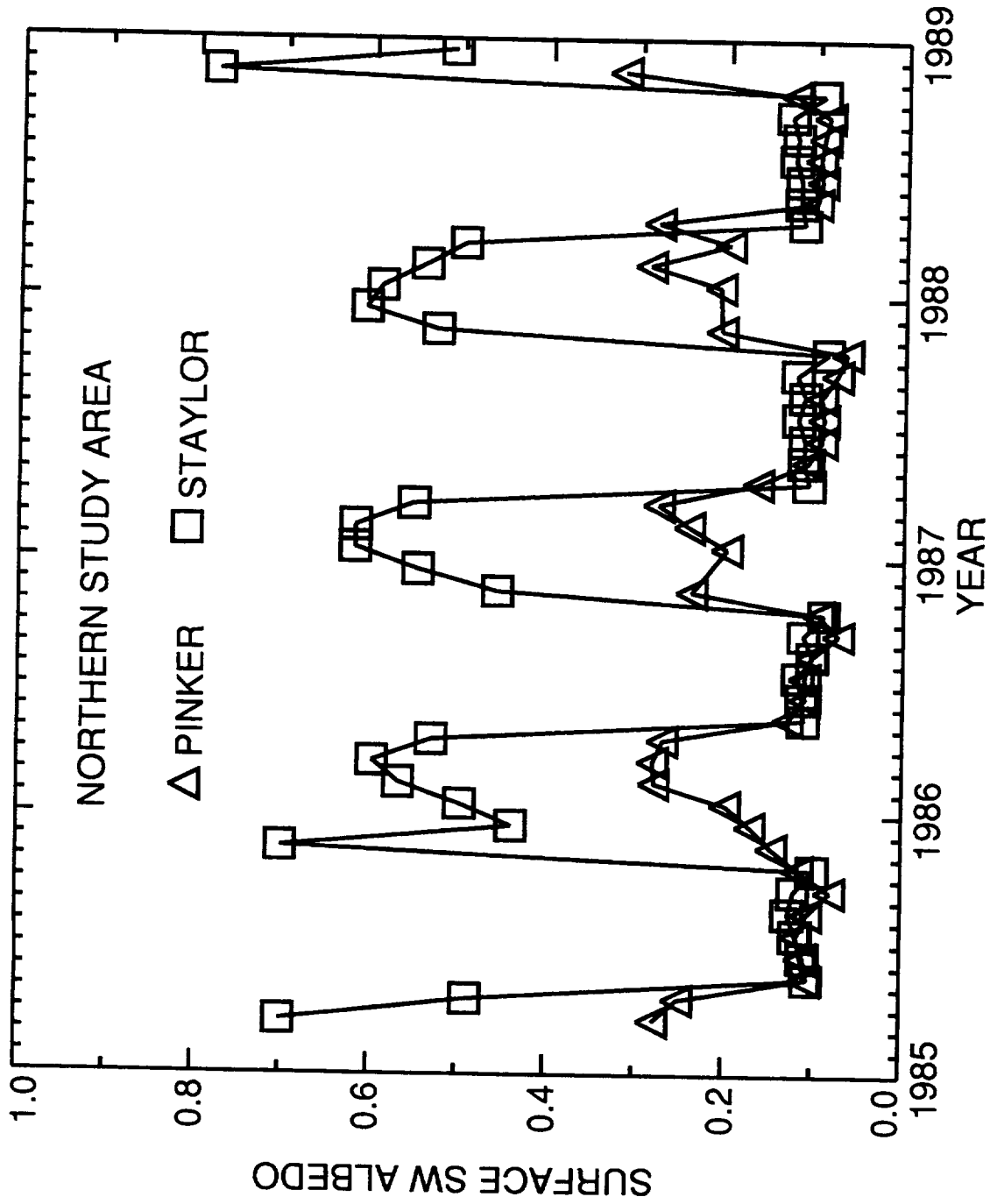


Figure 18. Surface SW albedo over the Northern Study Area.

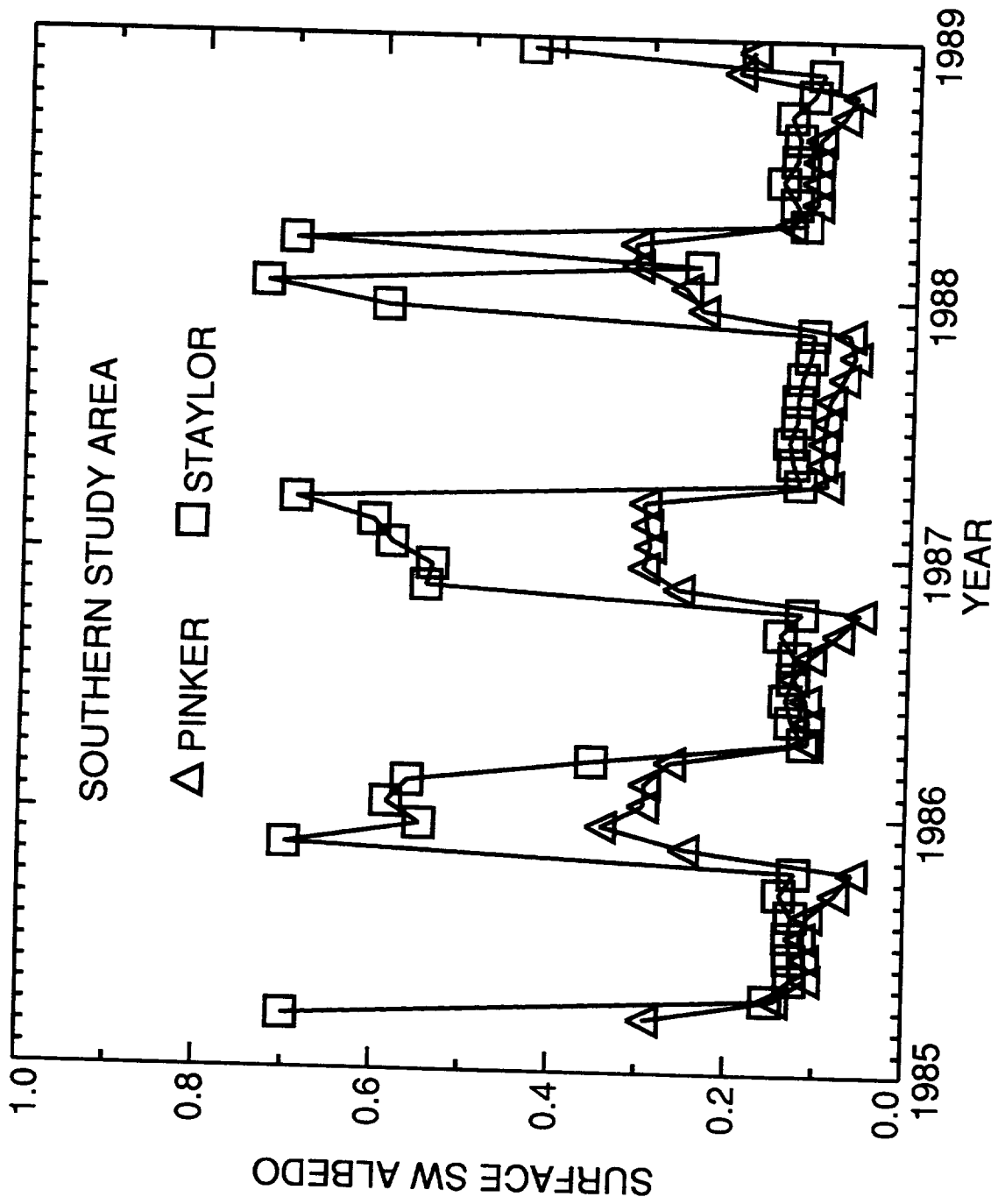


Figure 19. Surface SW albedo over the Southern Study Area.

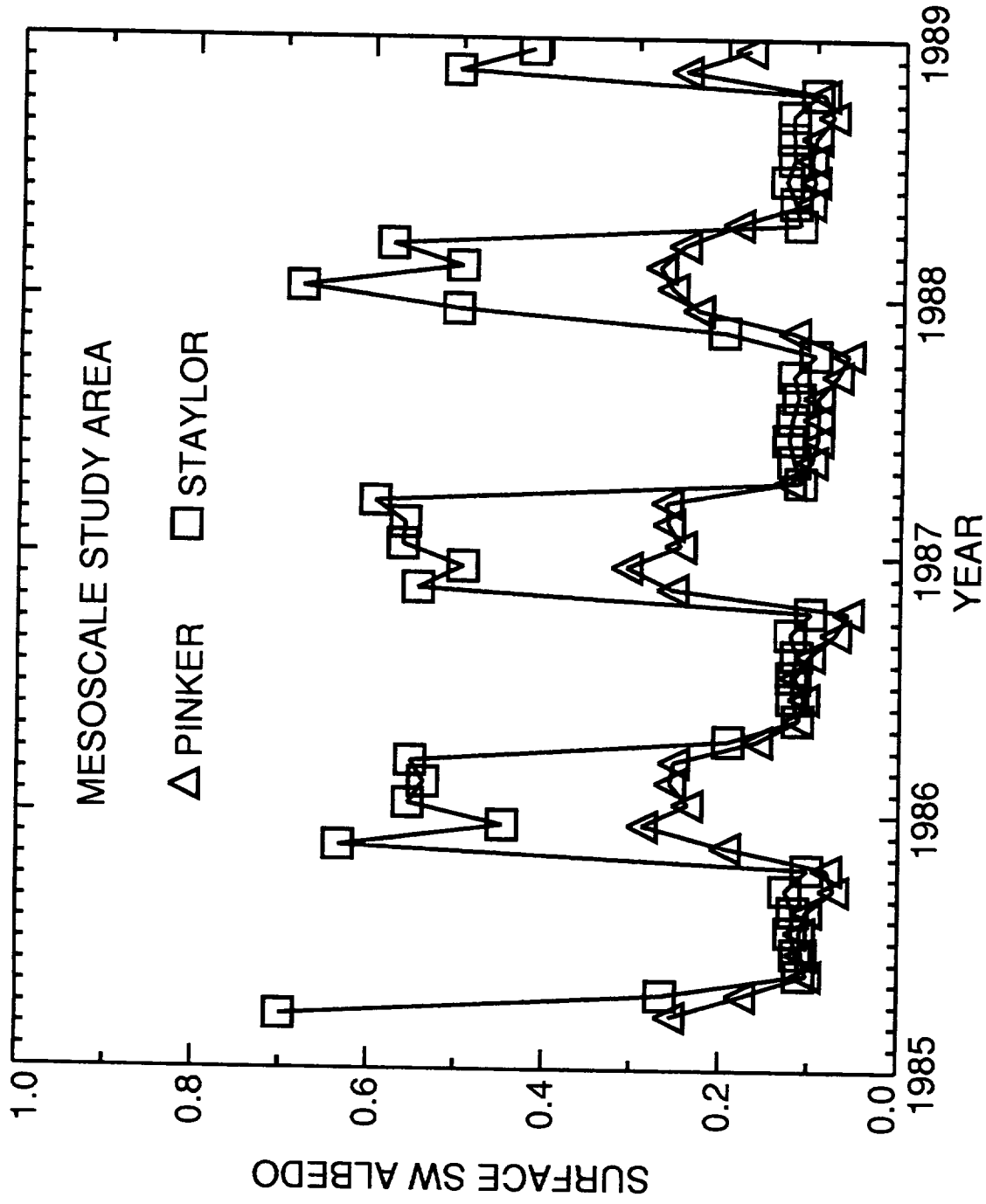


Figure 20. Surface SW albedo over the Mesoscale Study Area.

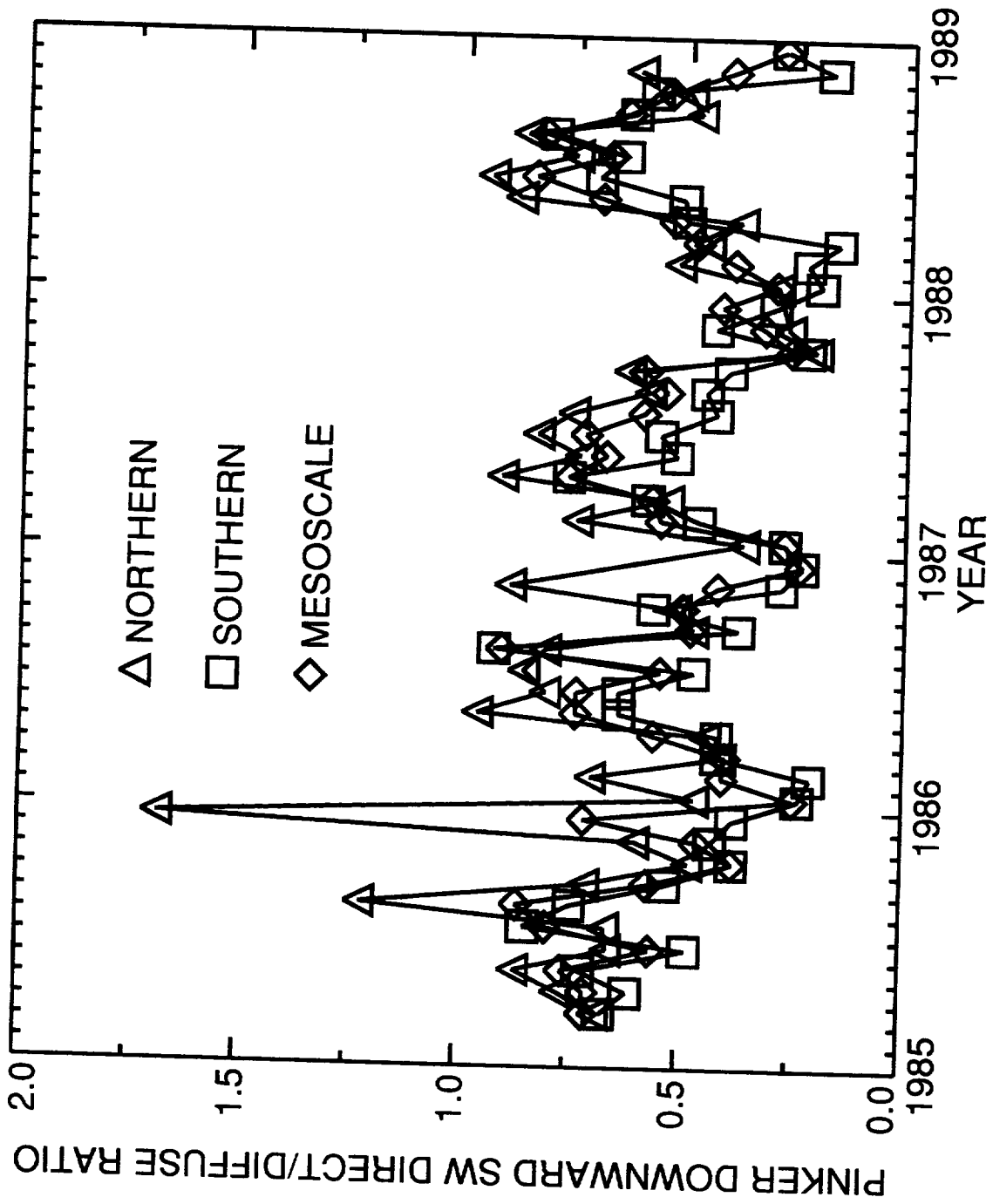


Figure 21. Pinker downward SW ratio of direct solar flux to diffuse skylight for each study area.

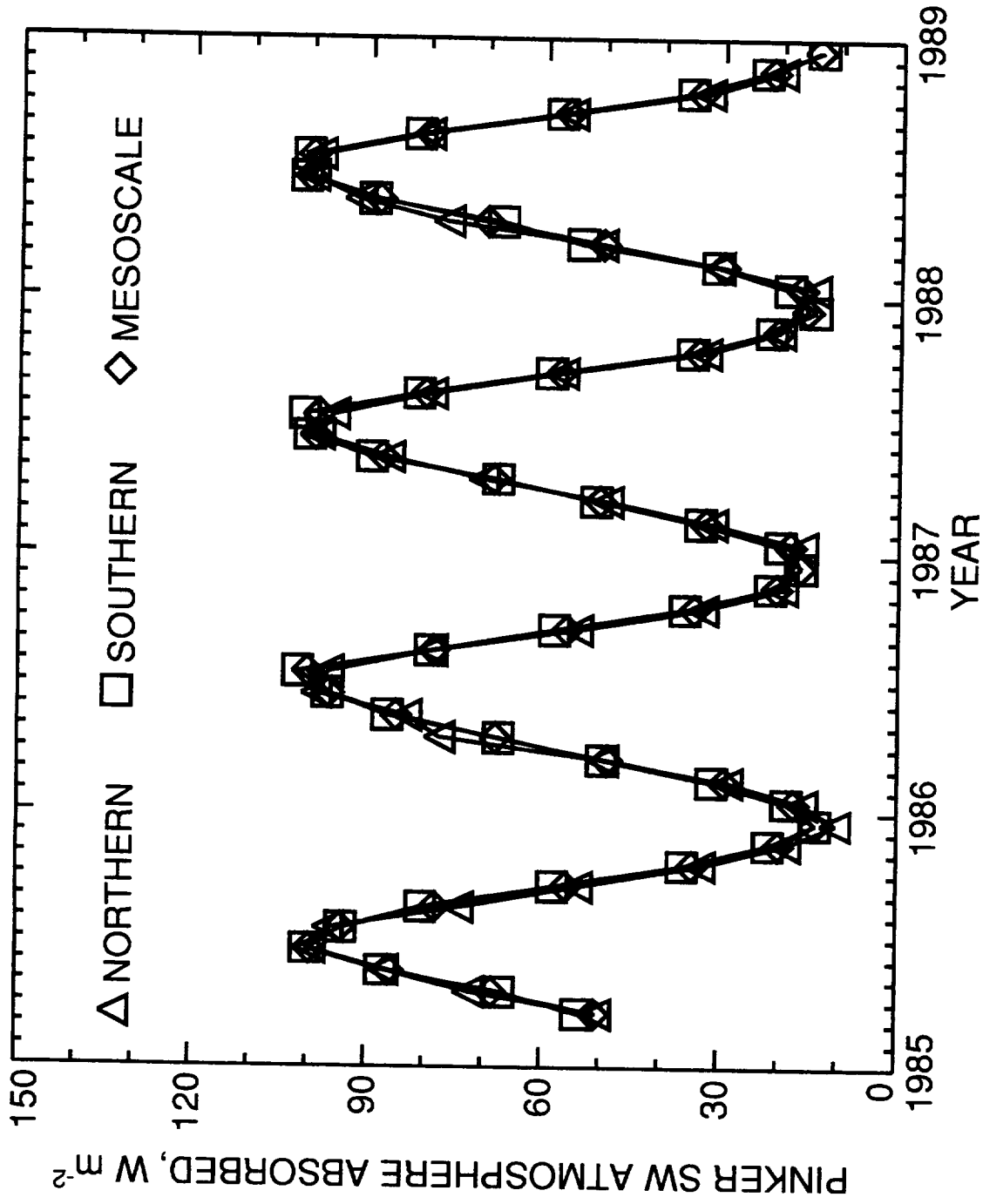


Figure 22. Pinker SW atmosphere absorbed flux for each study area.

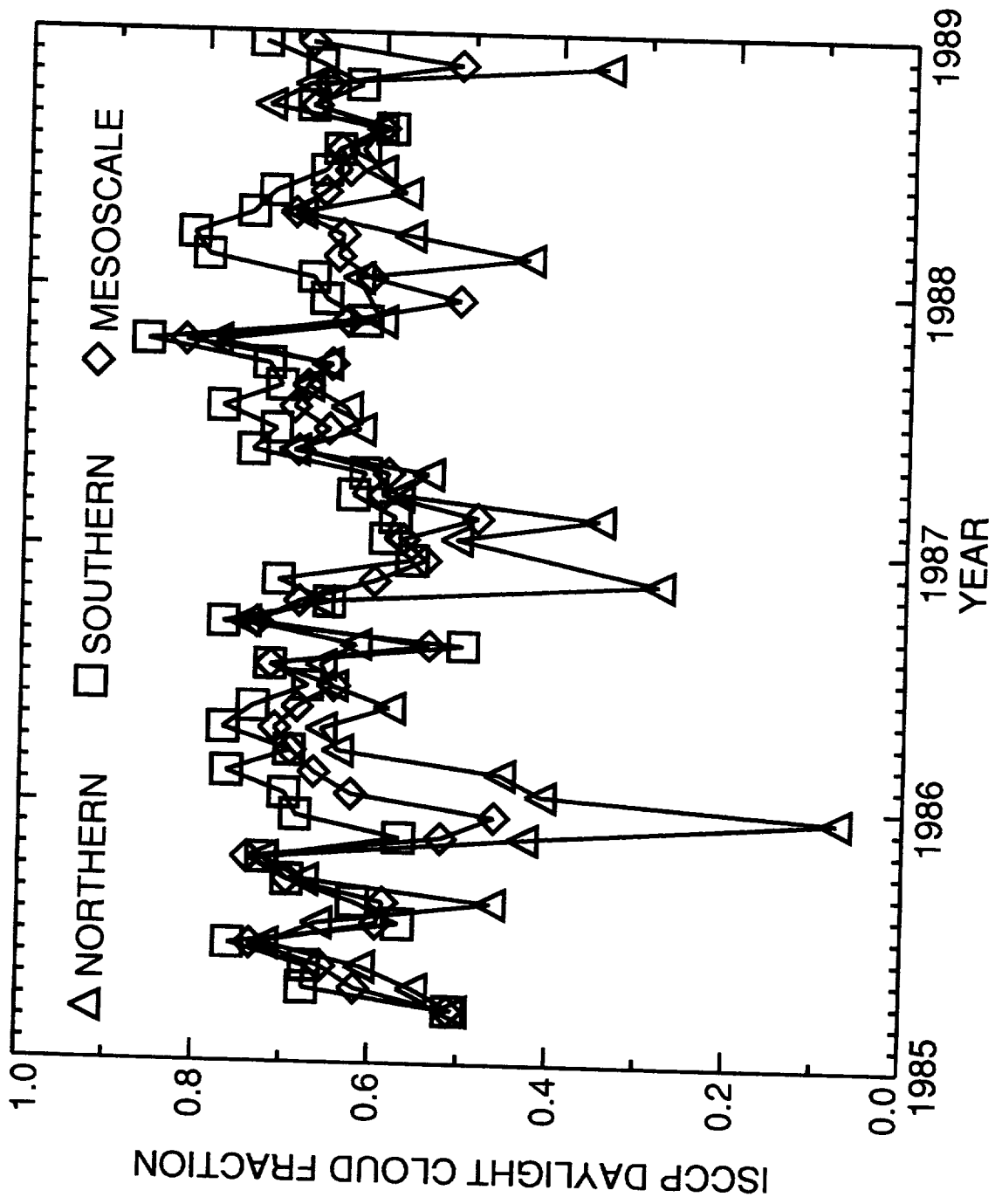


Figure 23. Average ISCCP daylight cloud fraction for each study area.

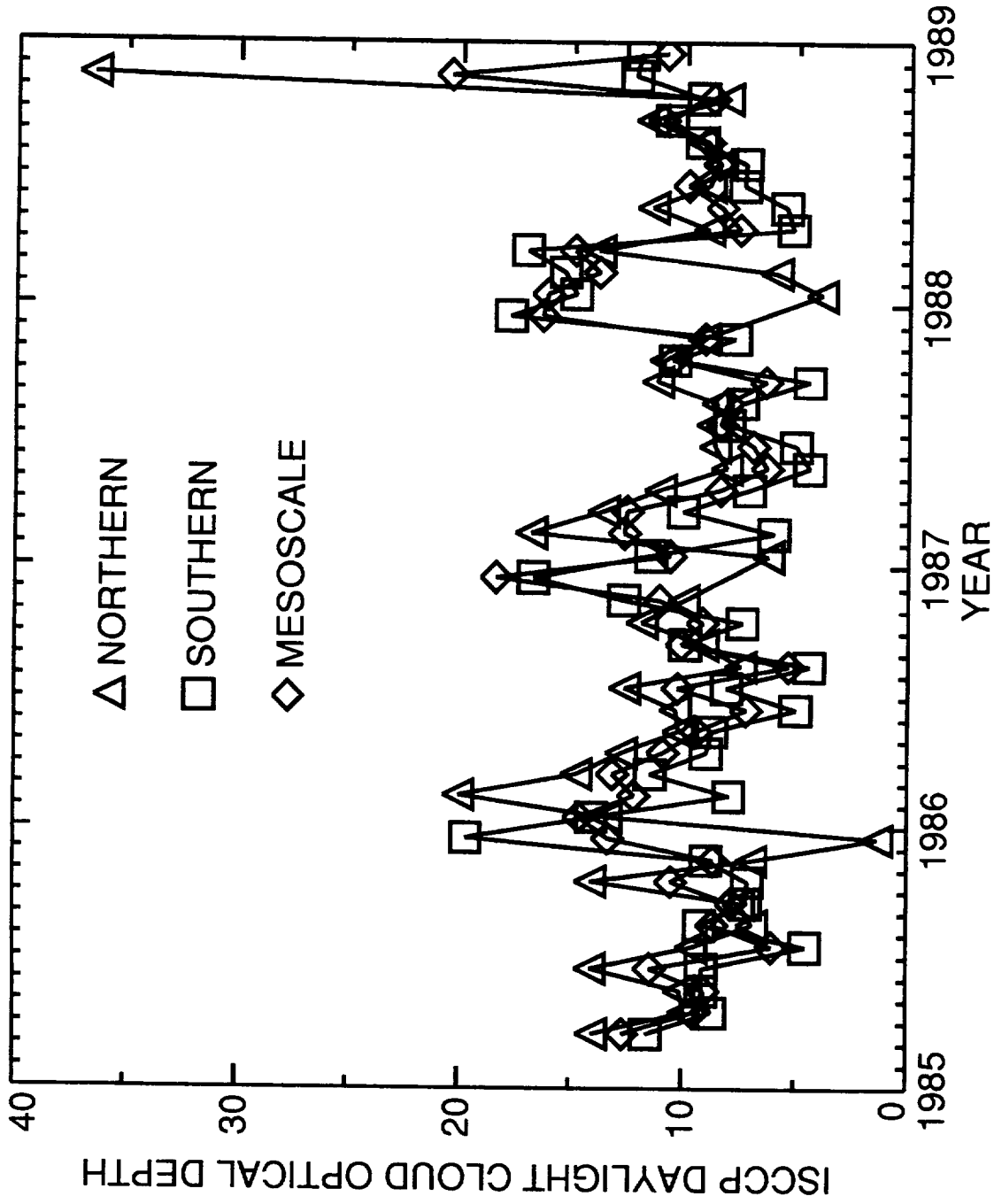


Figure 24. Average ISCCP daylight cloud optical depth for each study area.

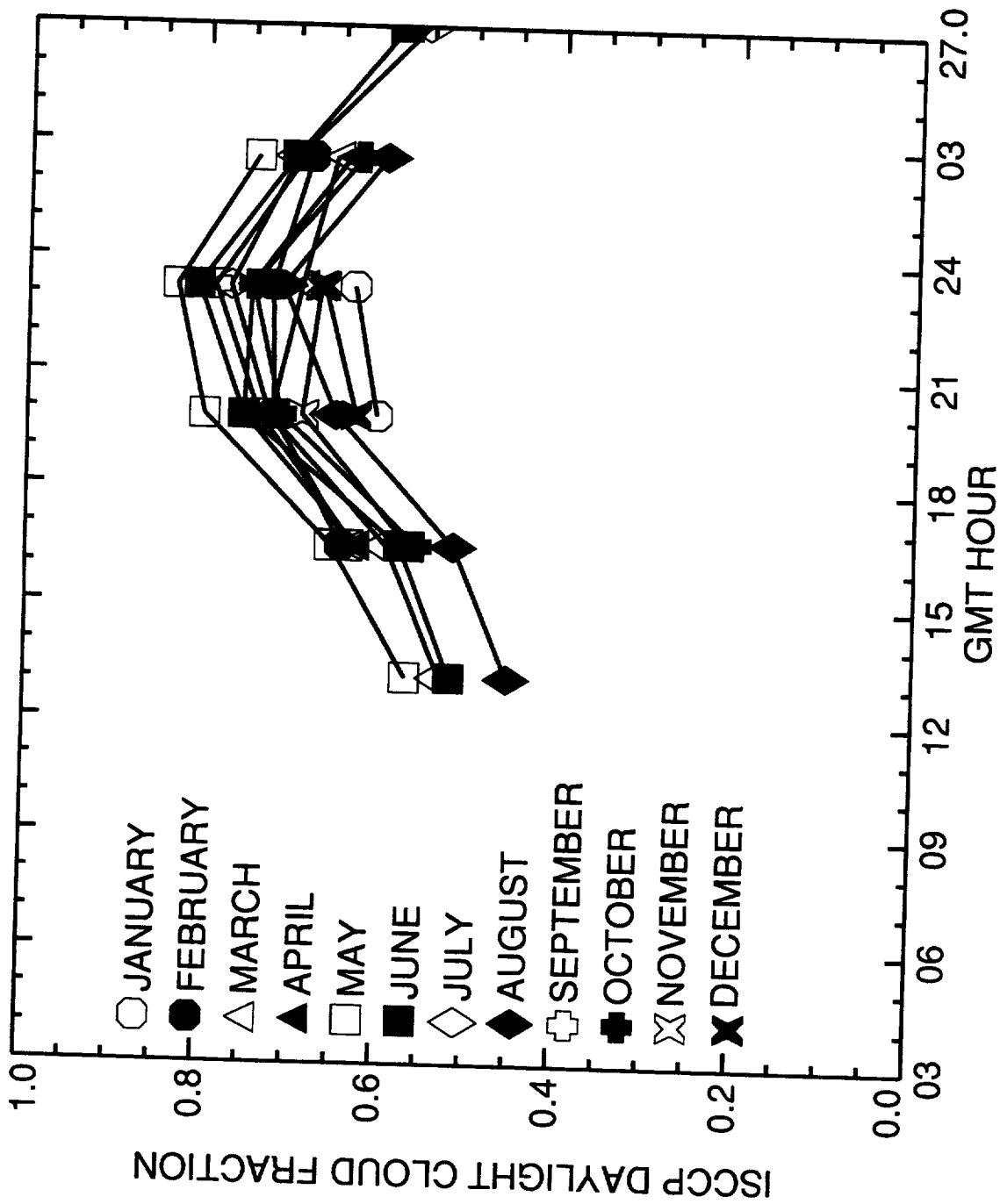


Figure 25. Average ISCCP daylight cloud fraction by month for Northern Study Area.

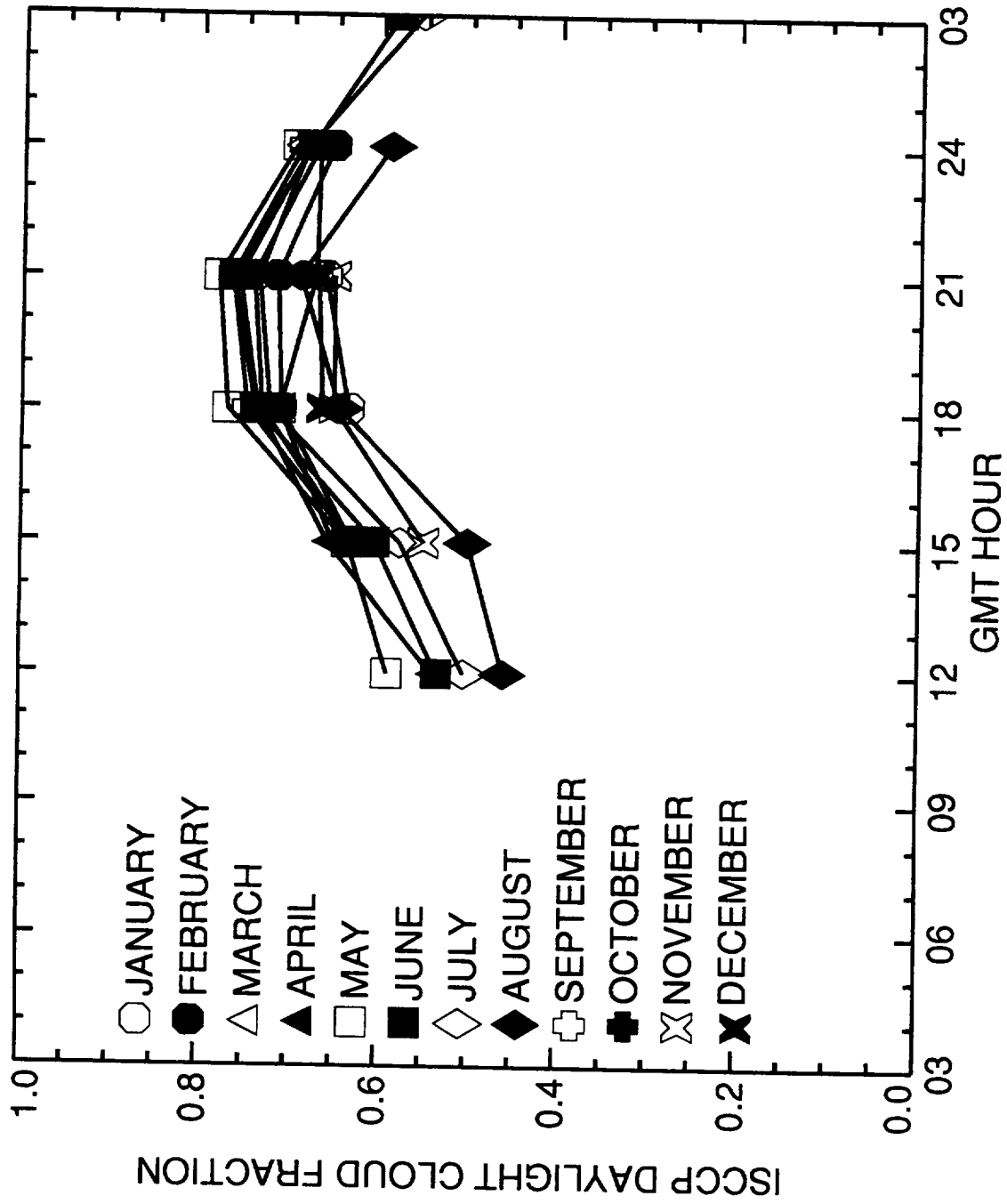


Figure 26. Average ISCCP daylight cloud fraction by month for Southern Study Area.

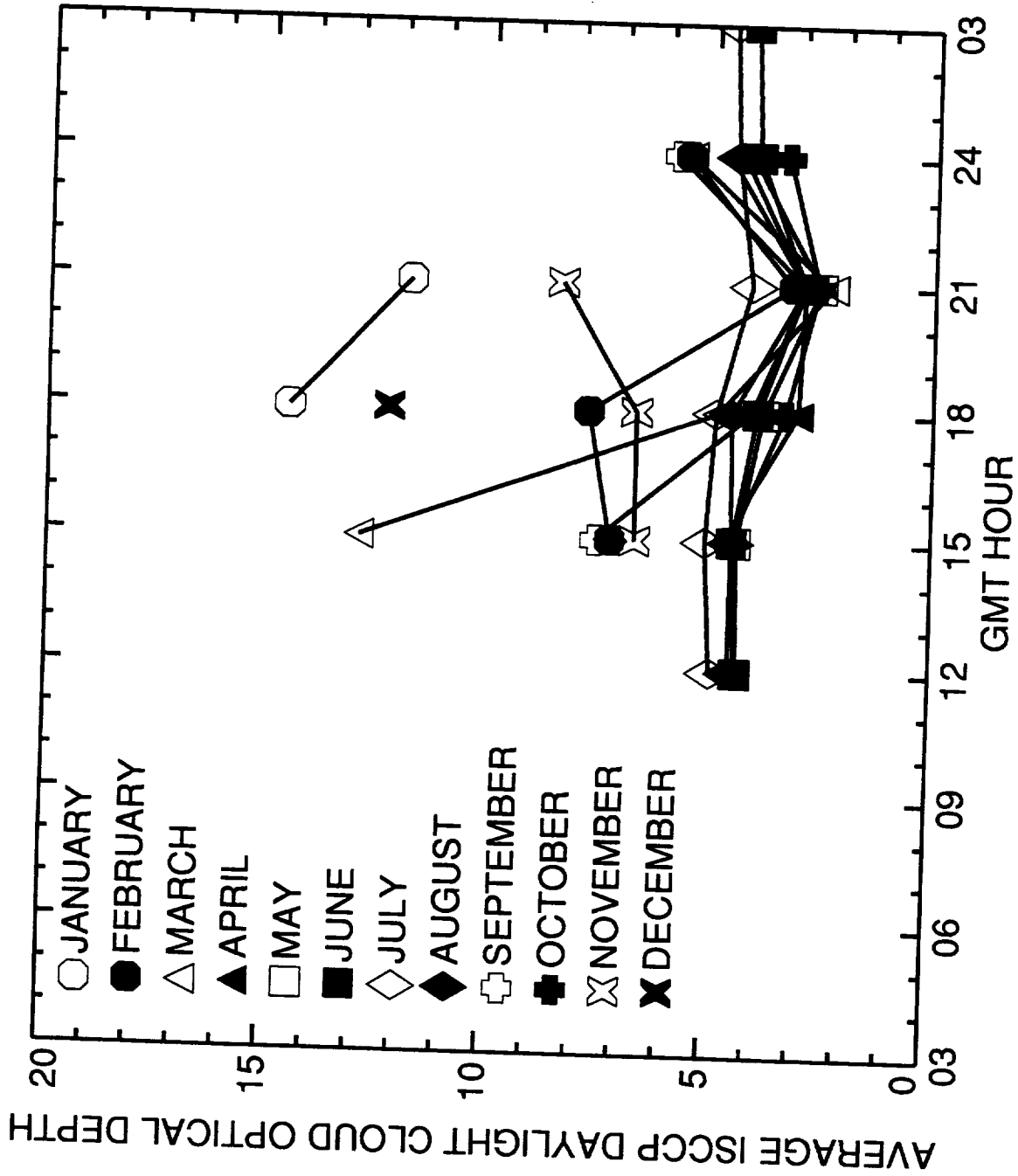


Figure 27. Average ISCCP daylight cloud optical depth by month for Northern Study Area.

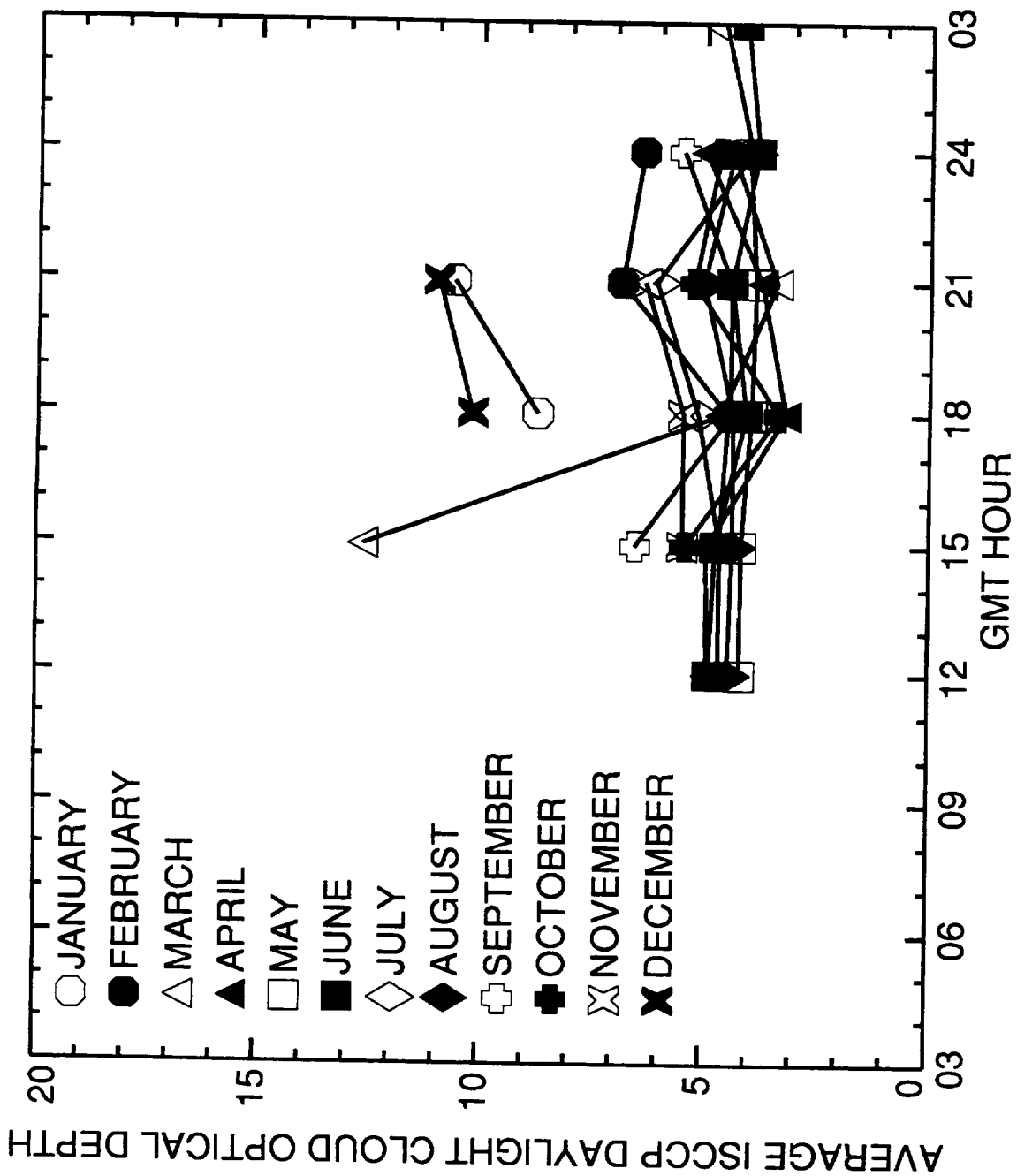


Figure 28. Average ISCCP daylight cloud optical depth by month for Southern Study Area.

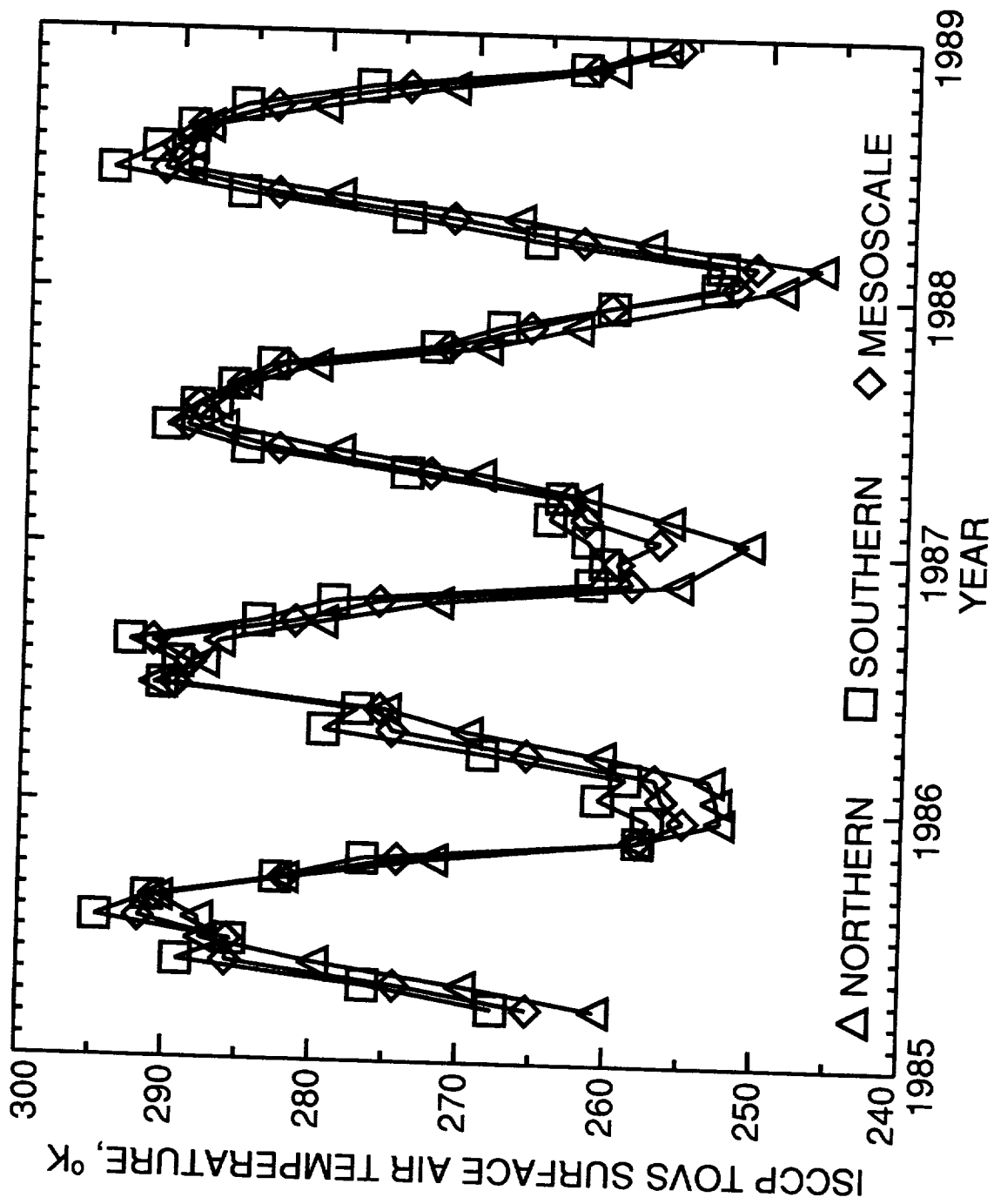


Figure 29. ISCCP TOVS surface air temperature for each study area.

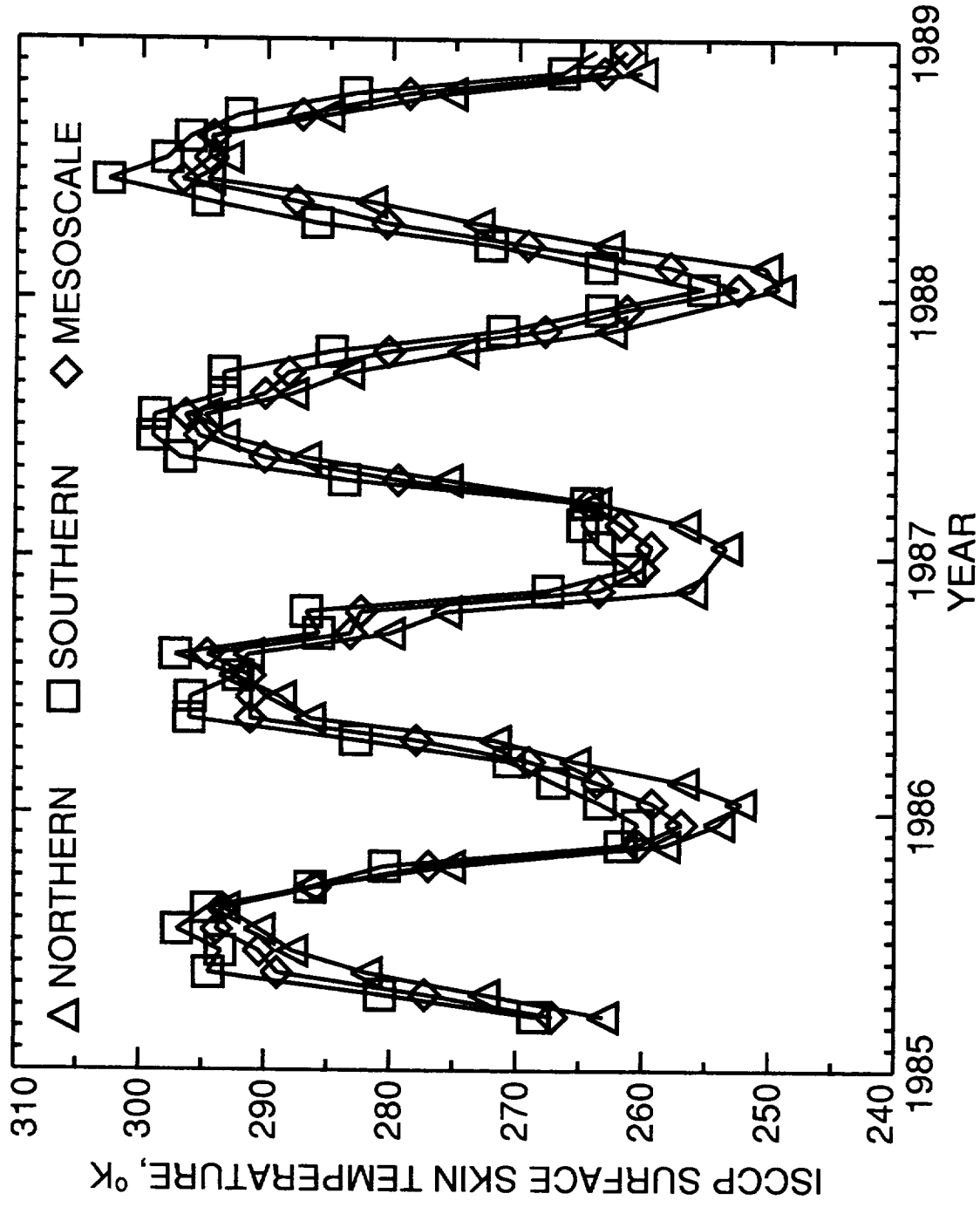


Figure 30. ISCCP surface skin temperature for each study area.

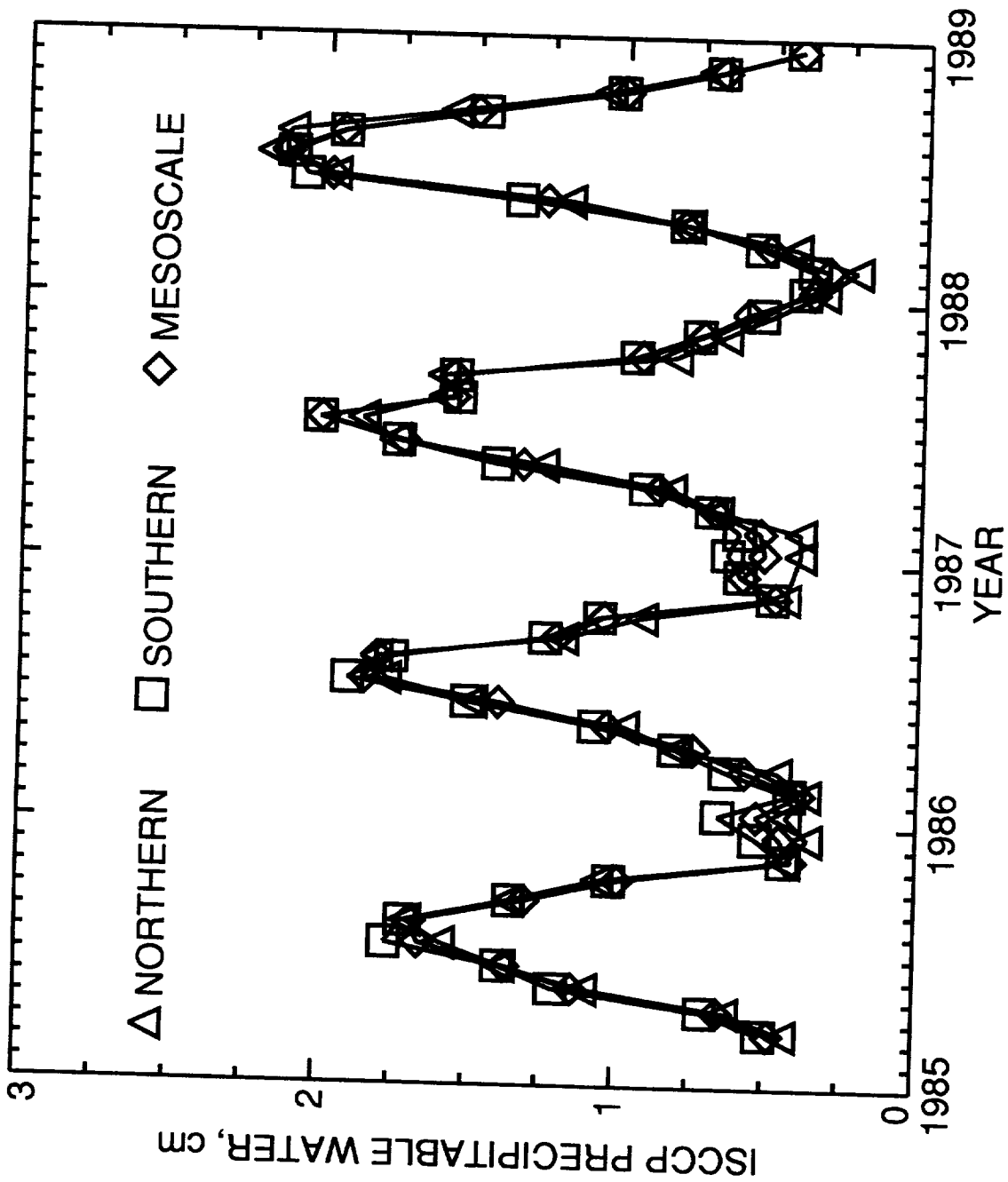


Figure 31. ISCCP column precipitable water for each study area.

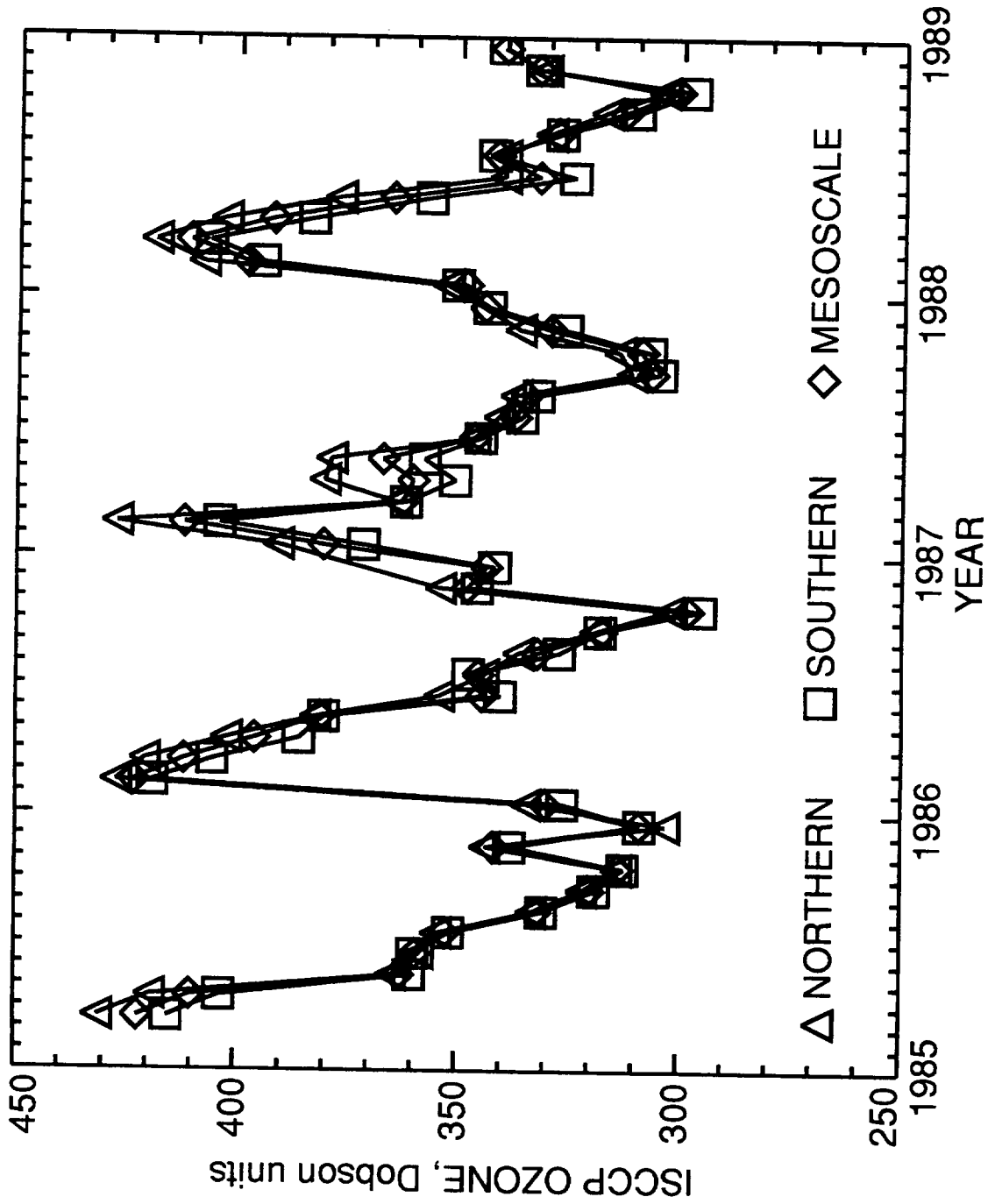


Figure 32. ISCCP column ozone for each study area.

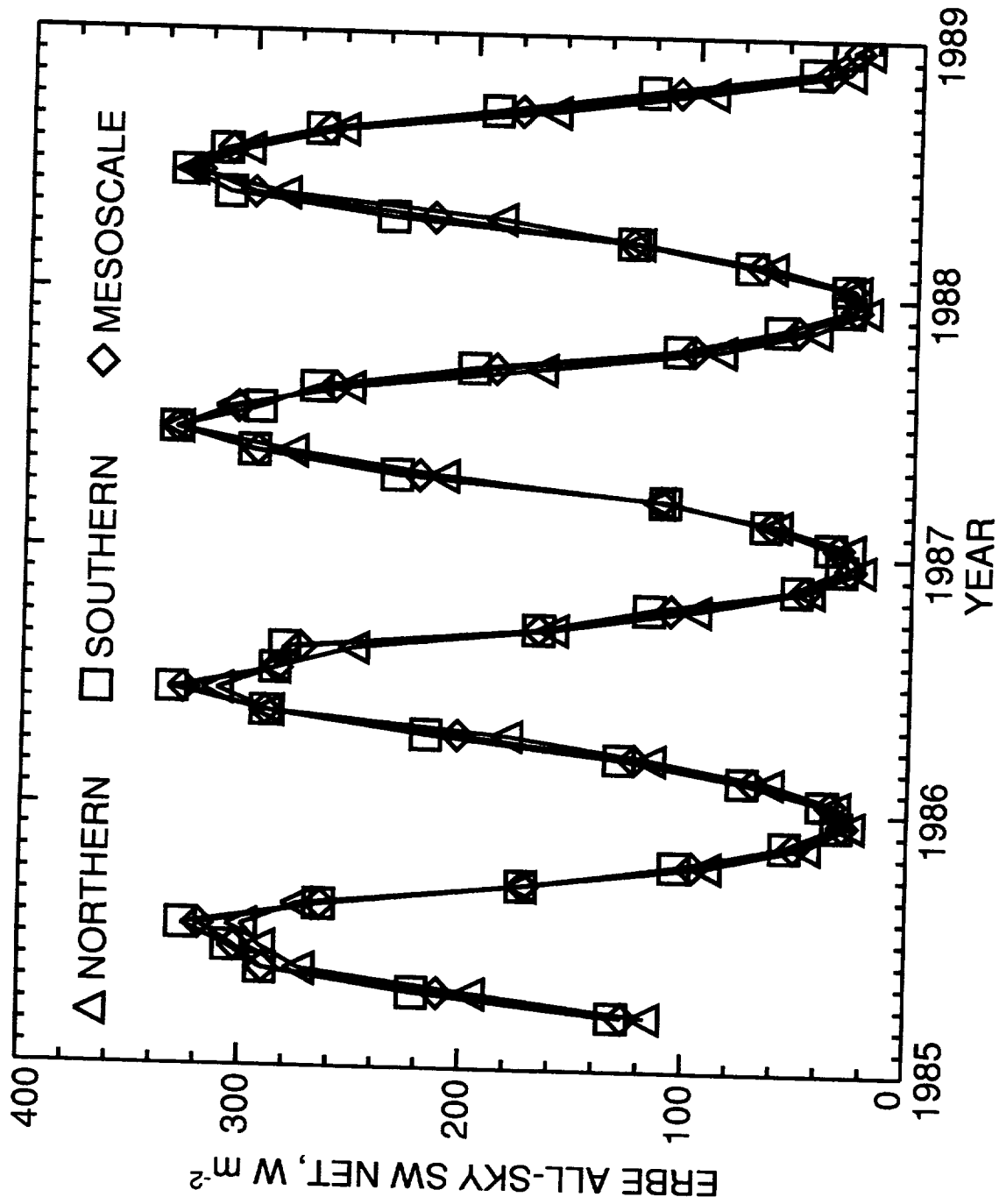


Figure 33. ERBE TOA all-sky SW net flux for each study area.

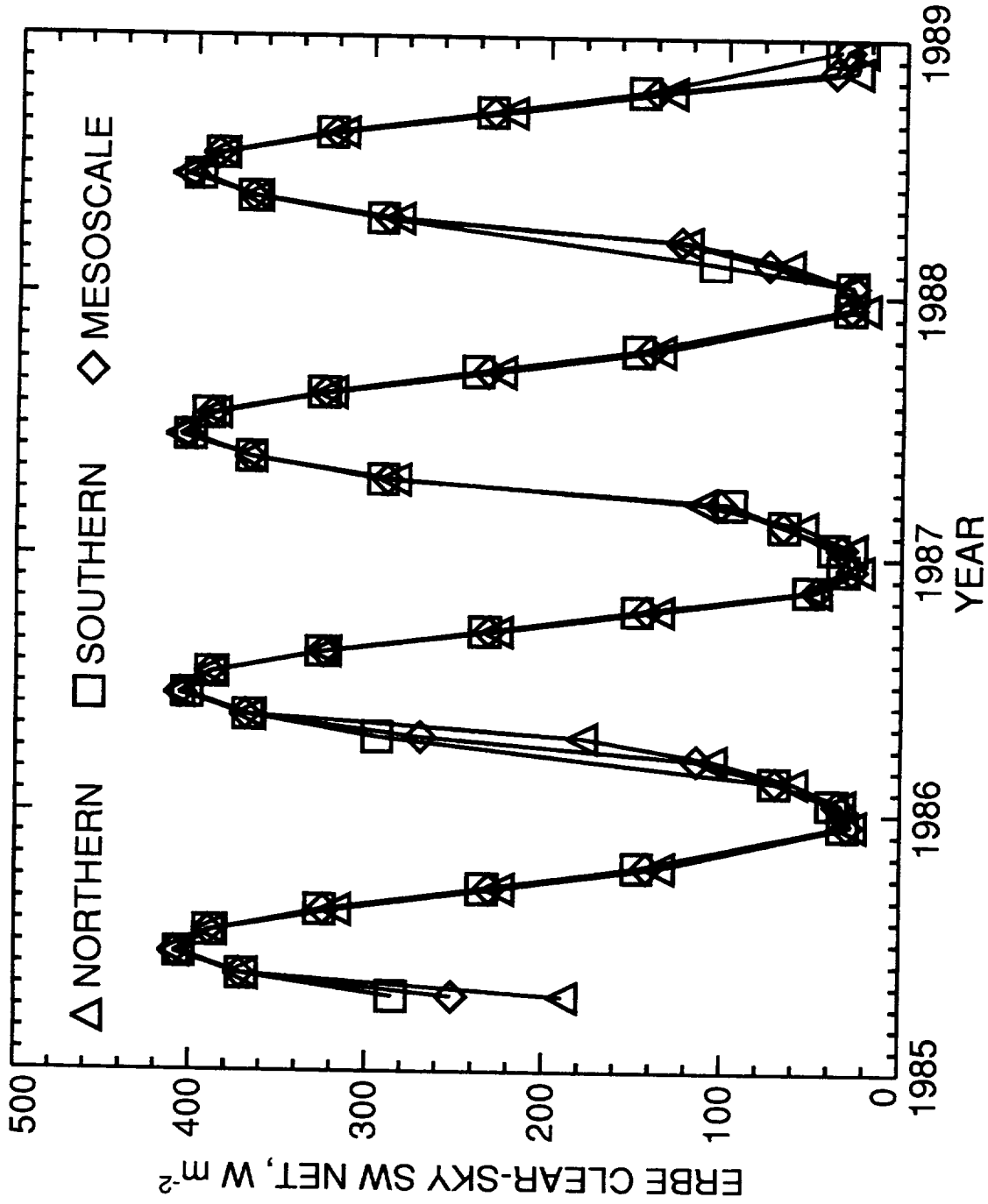


Figure 34. ERBE TOA clear-sky SW net flux for each study area.

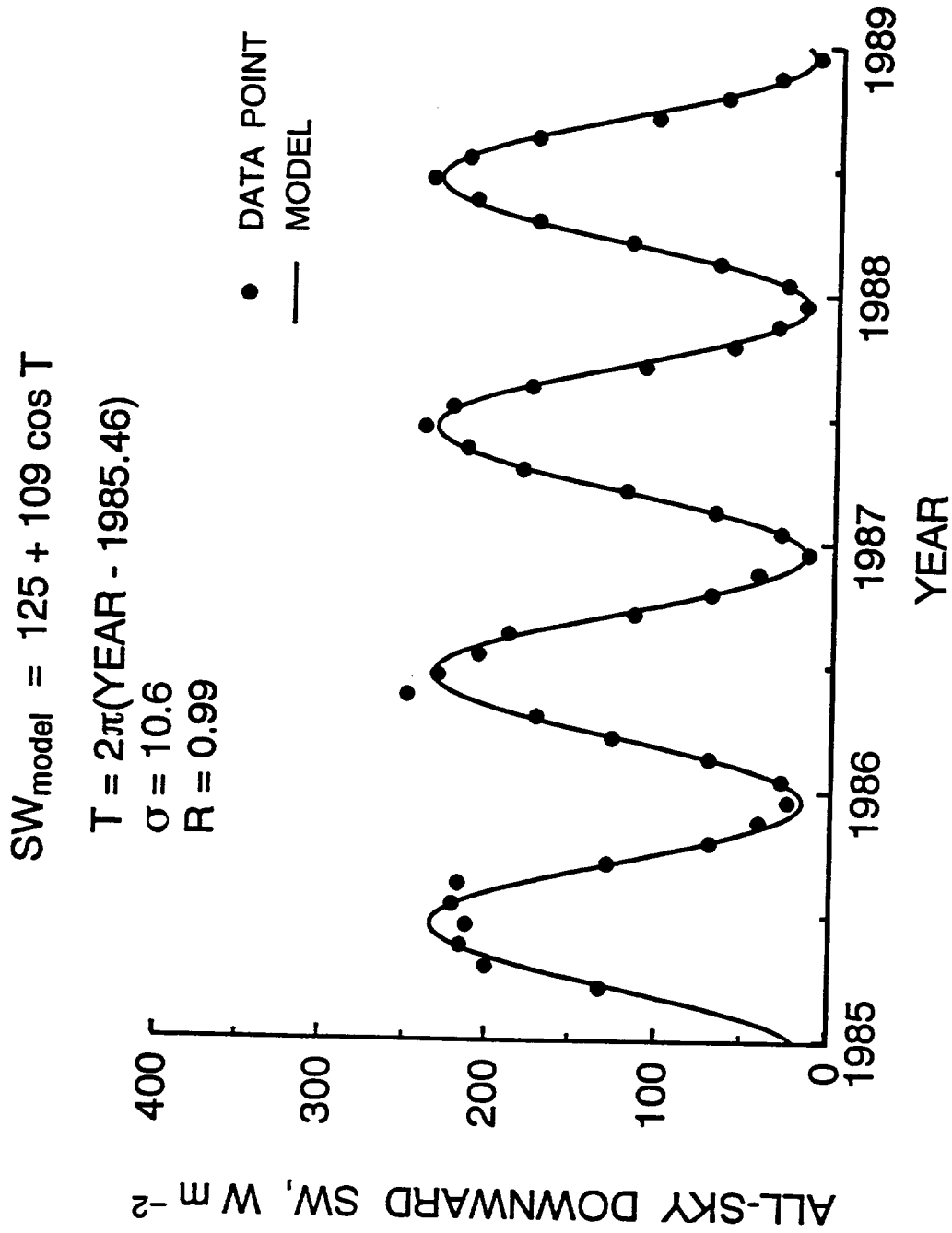


Figure 35. Curve fit to average of Pinker and Staylor surface all-sky downward SW flux for Northern Study Area.

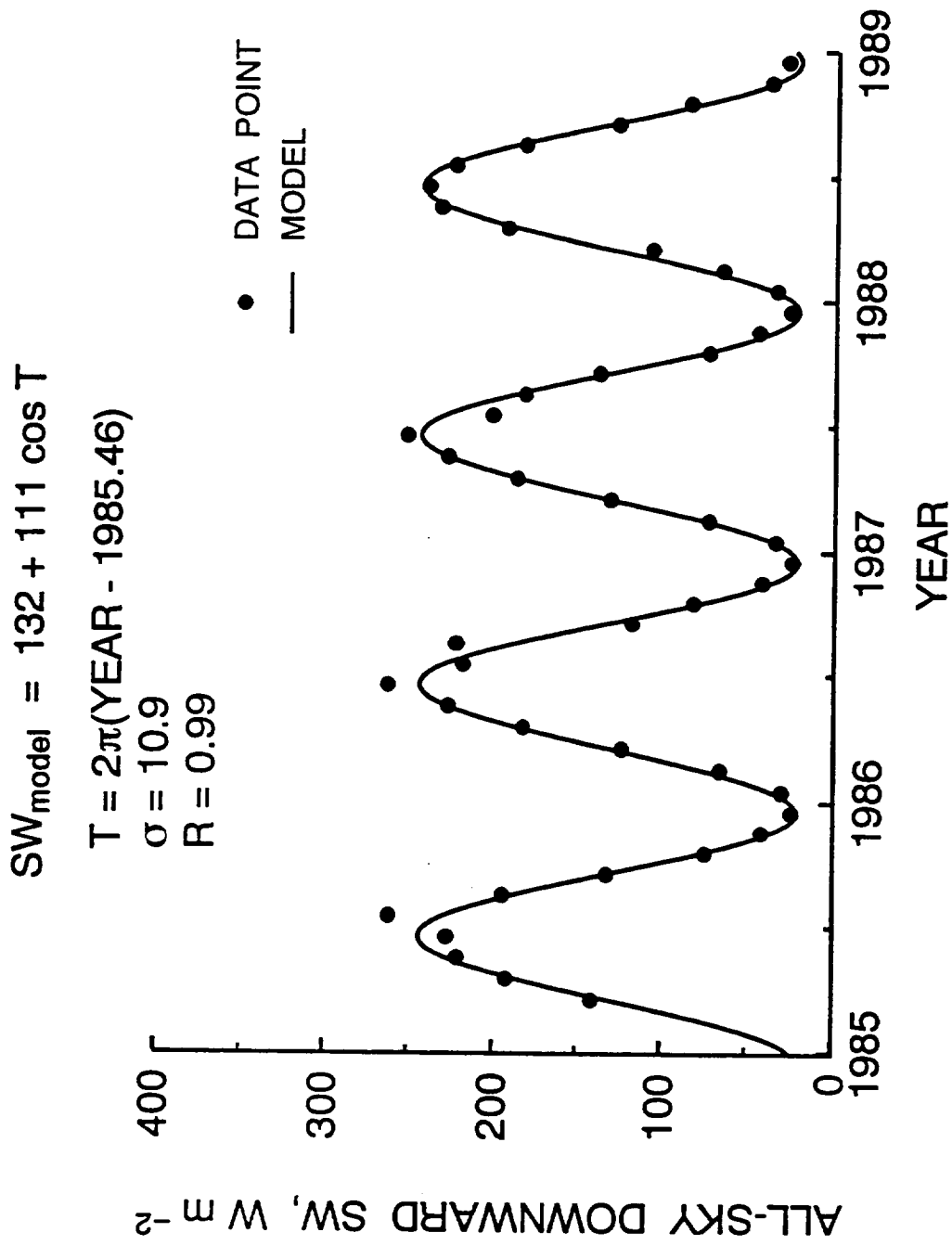


Figure 36. Curve fit to average of Pinker and Staylor surface all-sky downward SW flux for Southern Study Area.

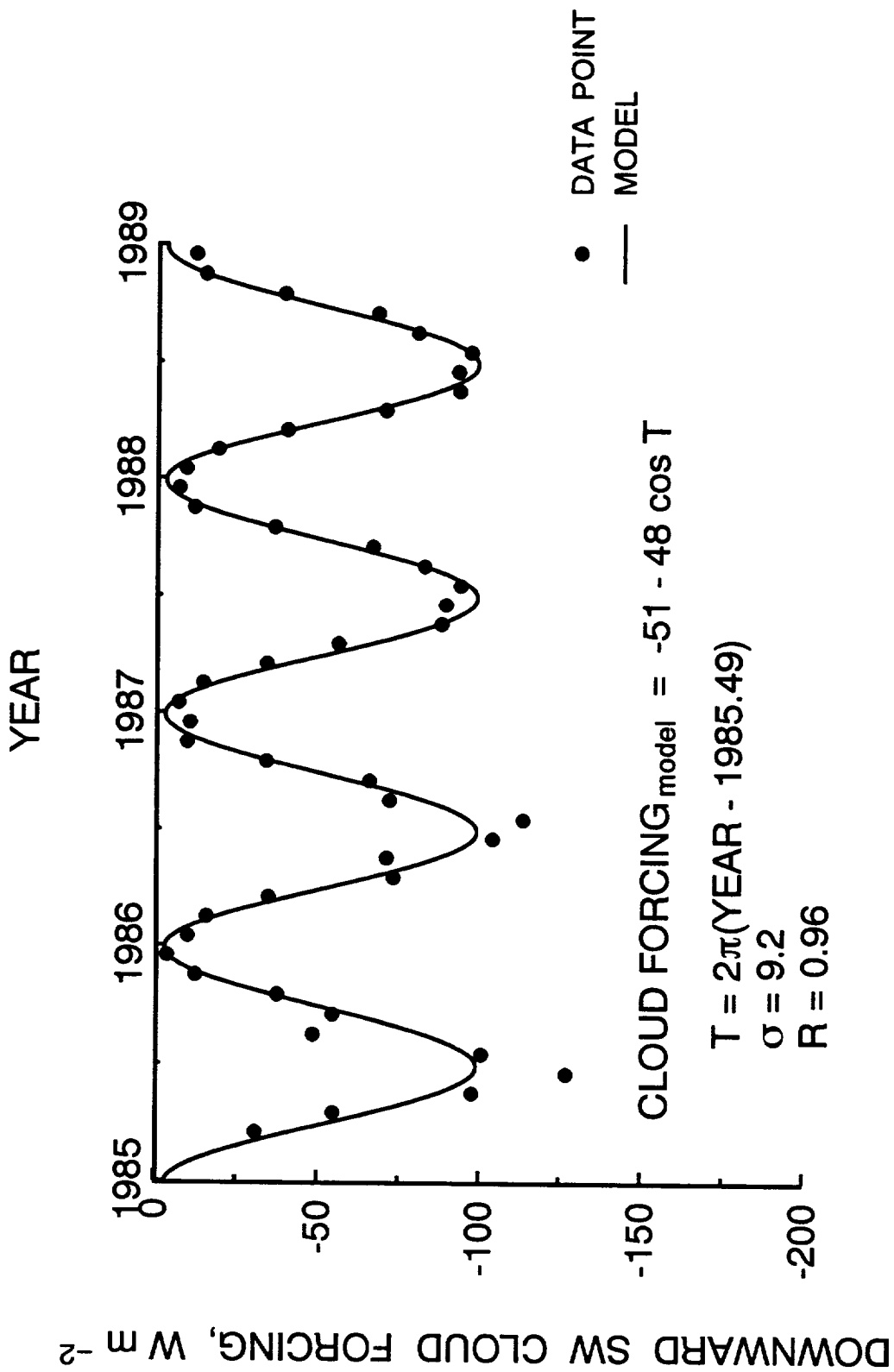


Figure 37. Curve fit to average of Pinker and Staylor surface downward SW cloud forcing for Northern Study Area.

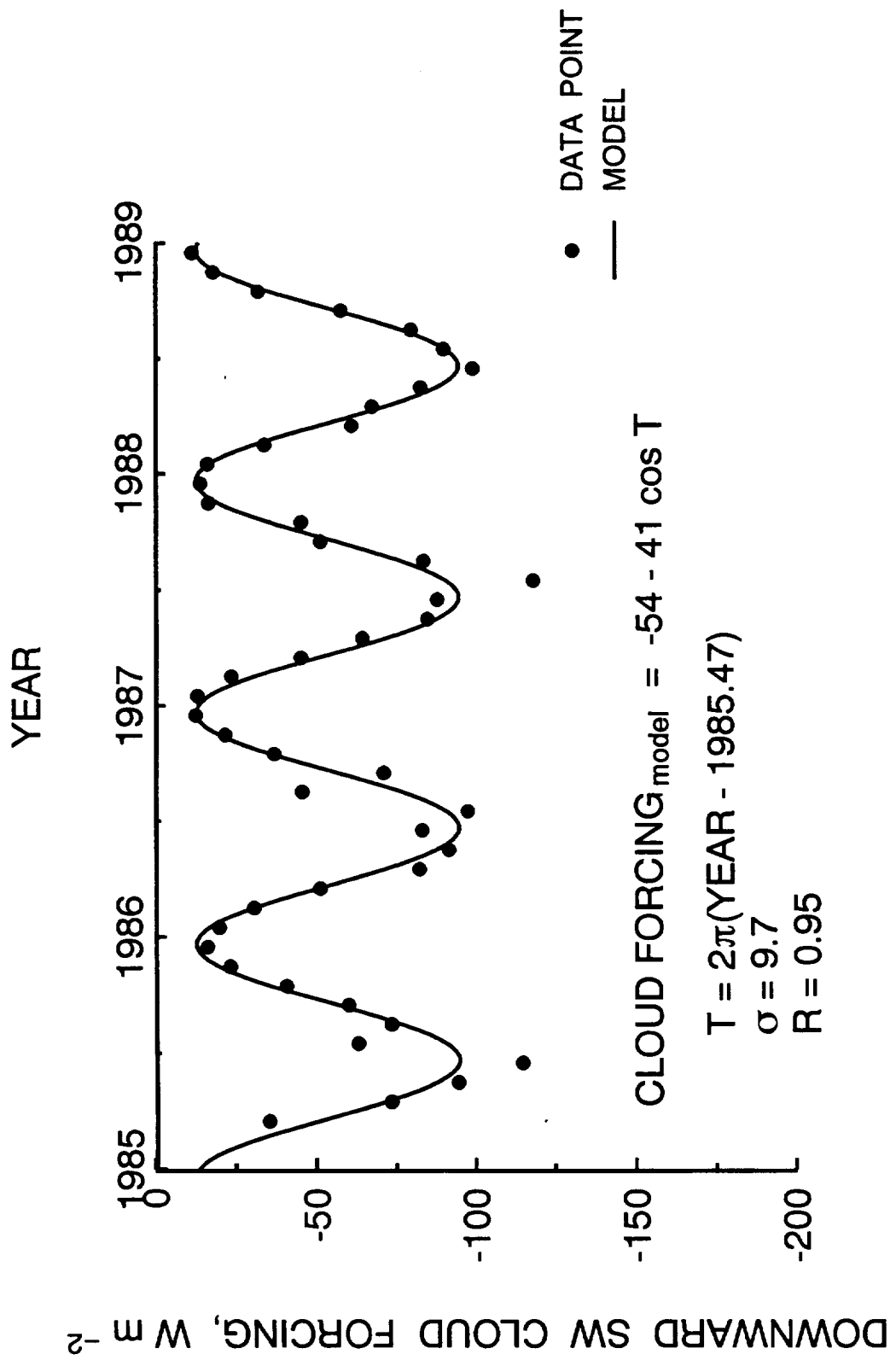


Figure 38. Curve fit to average of Pinker and Staylor surface downward SW cloud forcing for Southern Study Area.

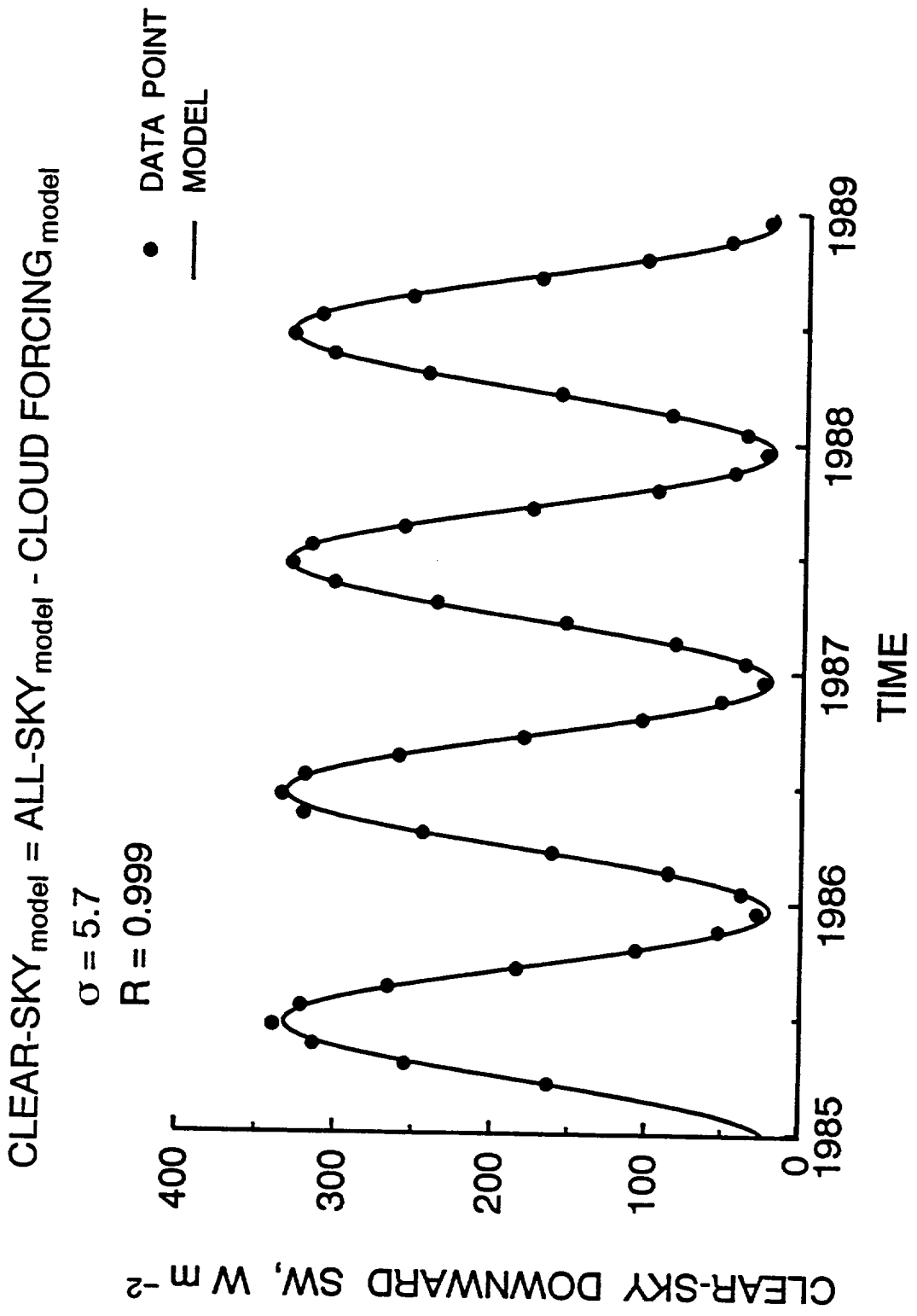


Figure 39. Curve fit to average of Pinker and Staylor surface clear-sky downward SW flux for Northern Study Area.

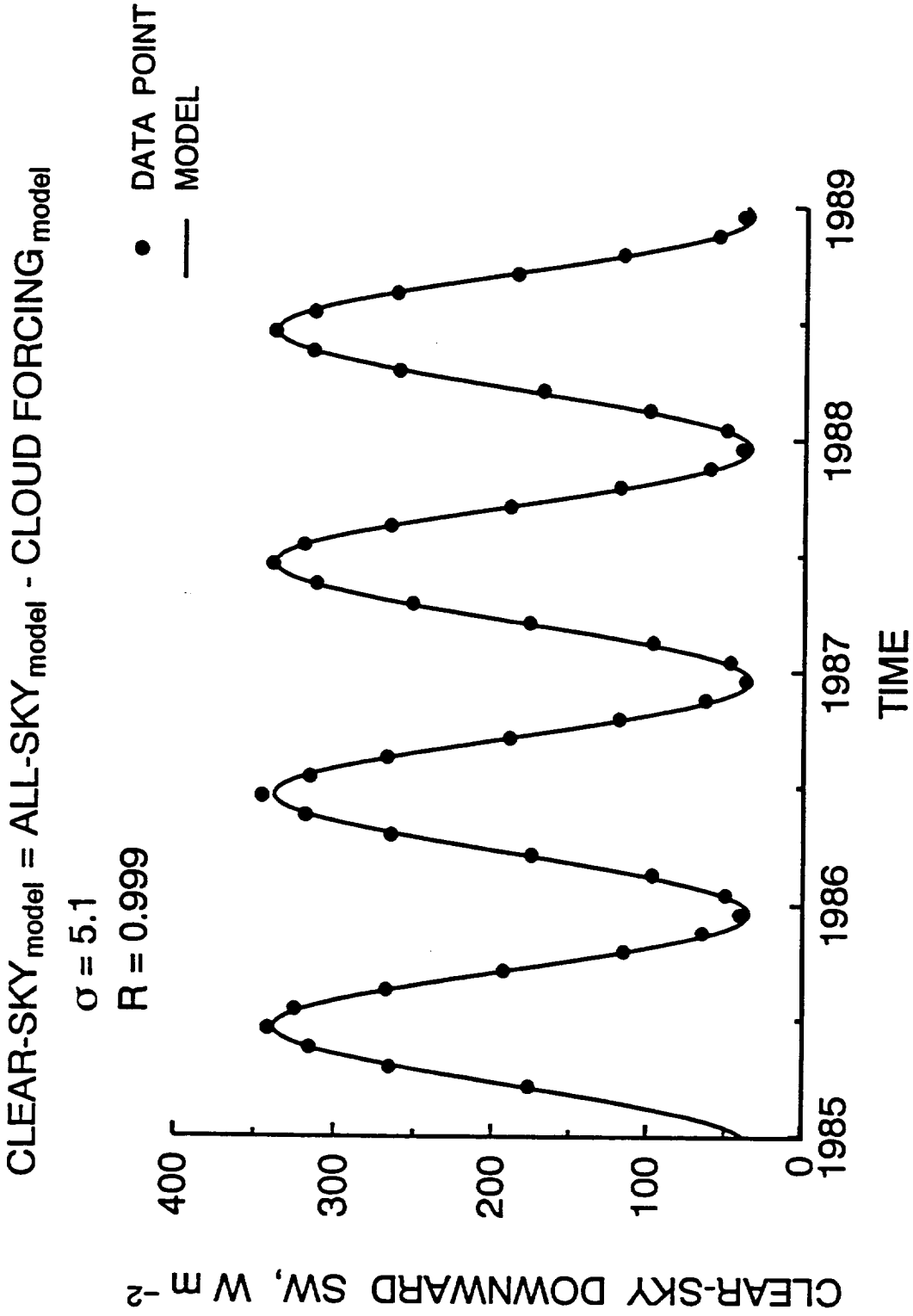


Figure 40. Curve fit to average of Pinker and Staylor surface clear-sky downward SW flux for Southern Study Area.

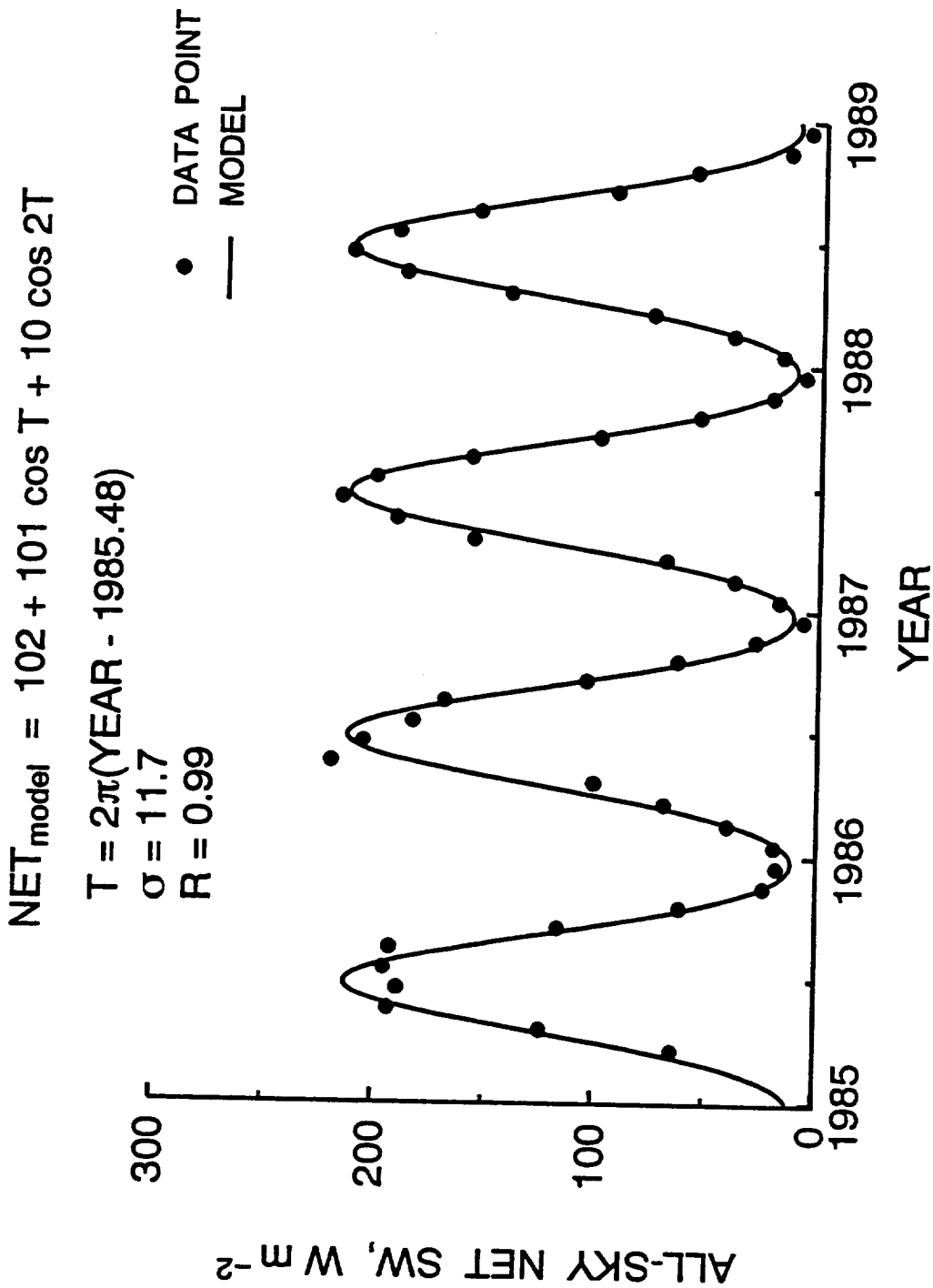


Figure 41. Curve fit to average of Pinker and Staylor surface all-sky net SW flux for Northern Study Area.

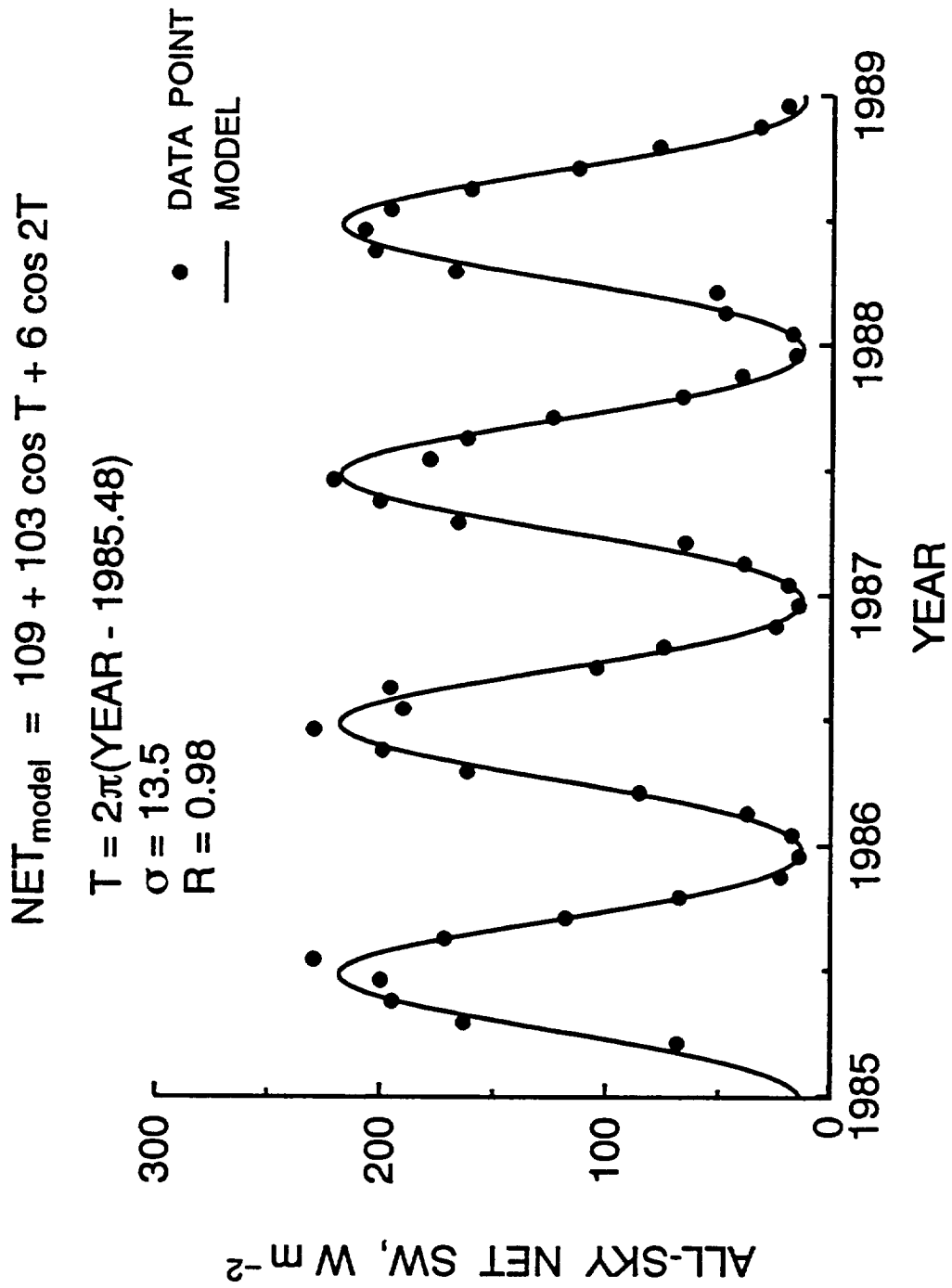


Figure 42. Curve fit to average of Pinker and Staylor surface all-sky net SW flux for Southern Study Area.

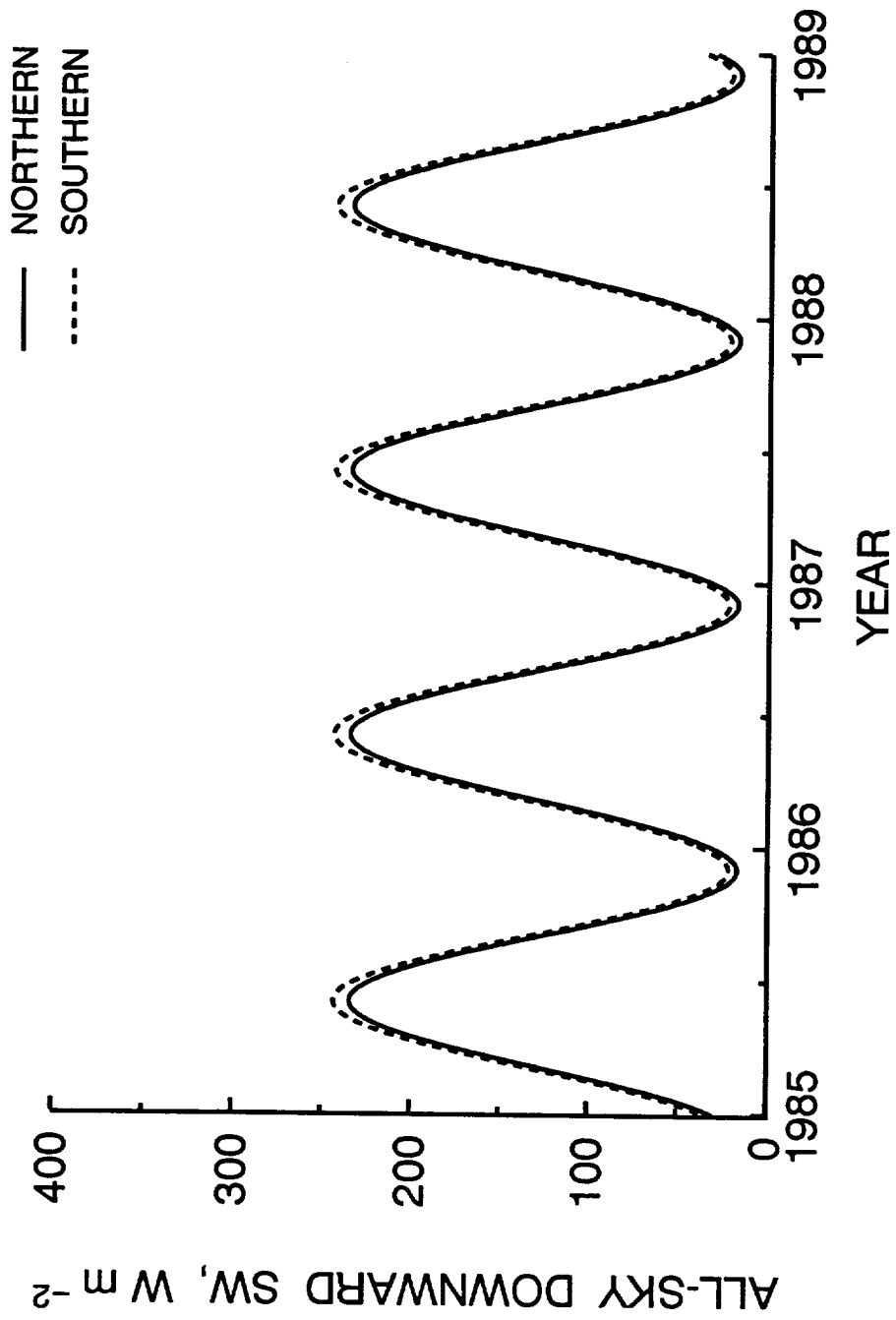


Figure 43. All-sky downward SW flux for Northern and Southern Study Areas from 1985-89.

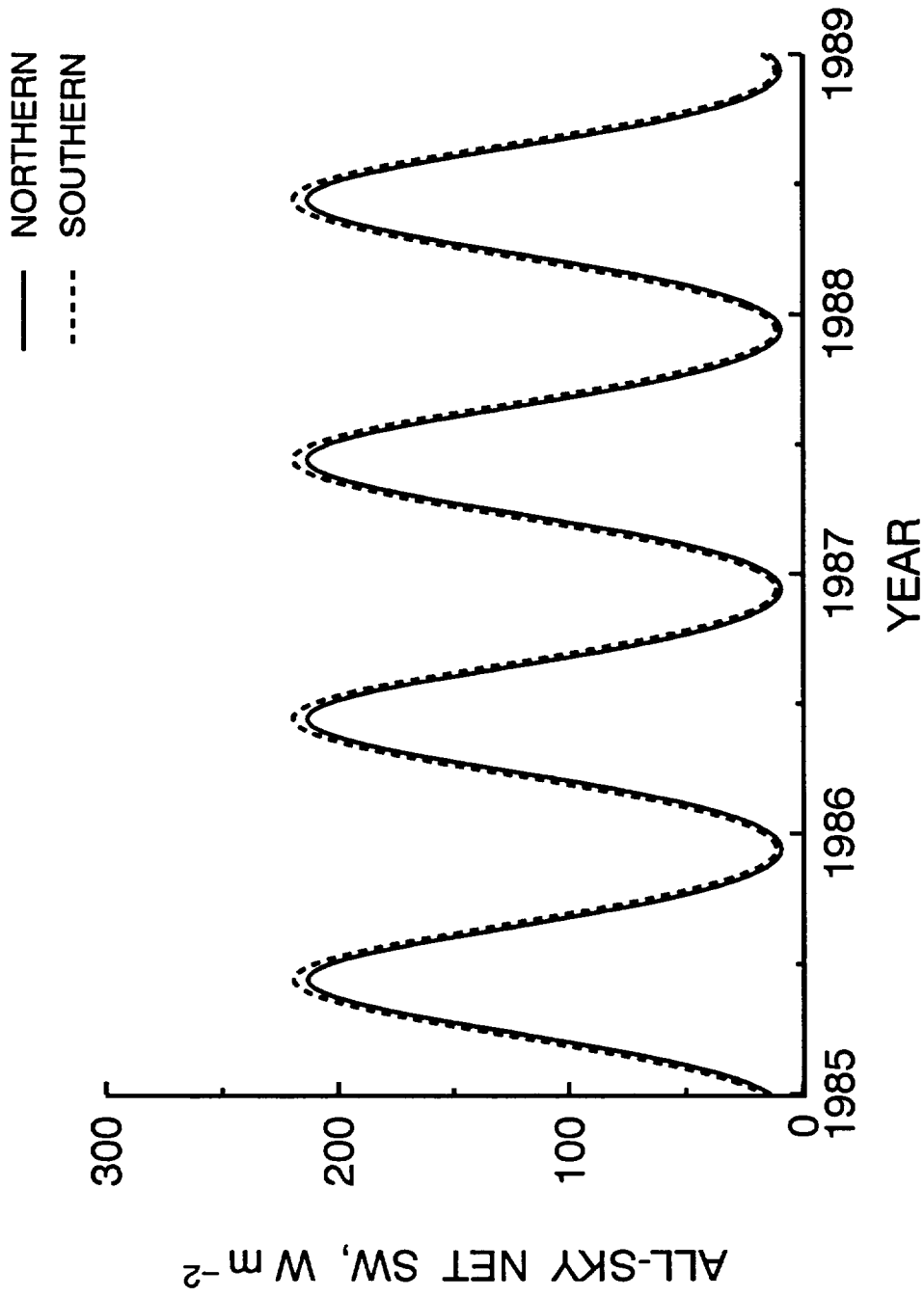


Figure 44. All-sky net SW flux for Northern and Southern Study Areas from 1985-89.

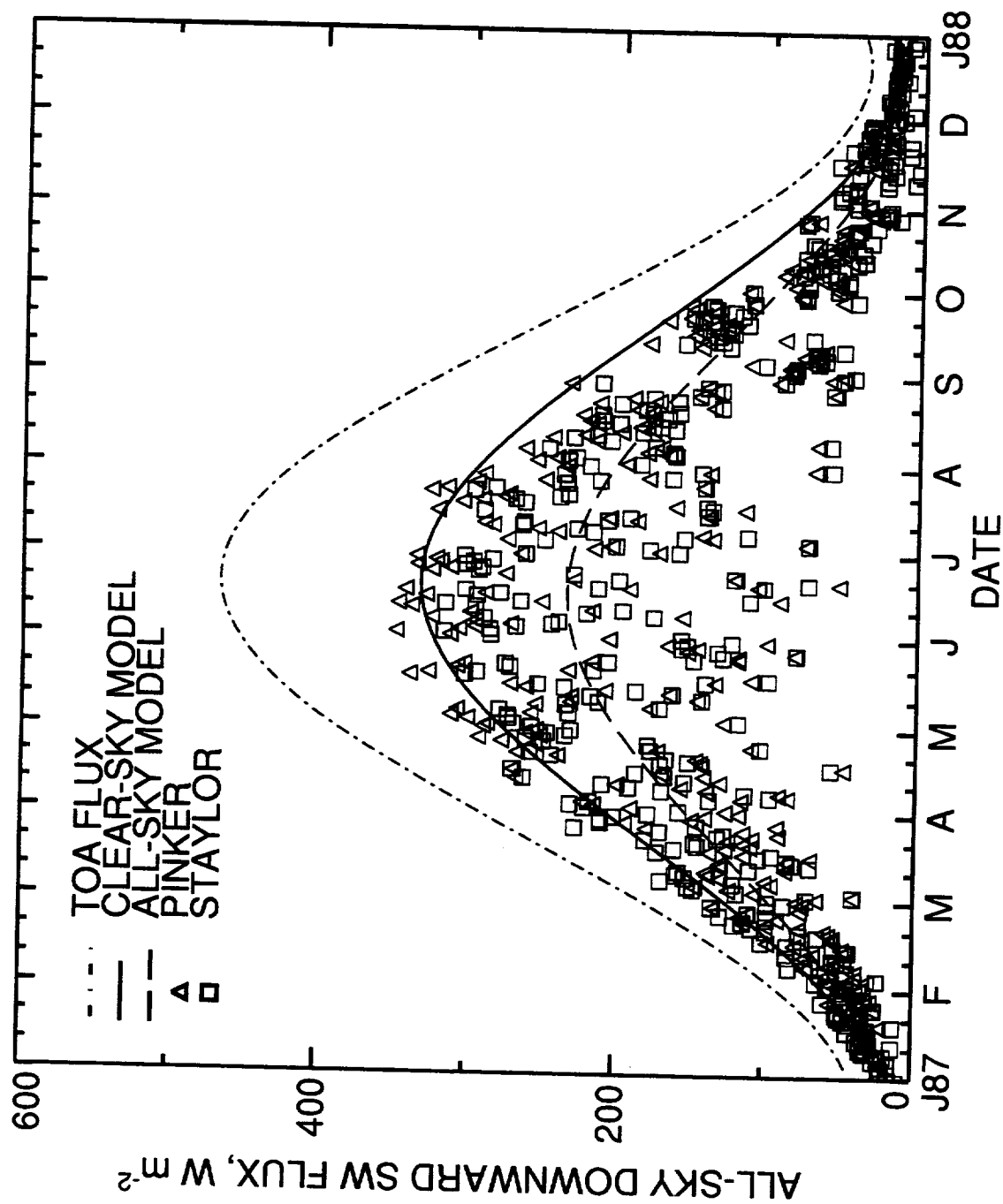


Figure 45. Clear-sky, all-sky and TOA monthly downward SW flux compared to Pinker and Staylor daily all-sky results for the Northern Study Area.

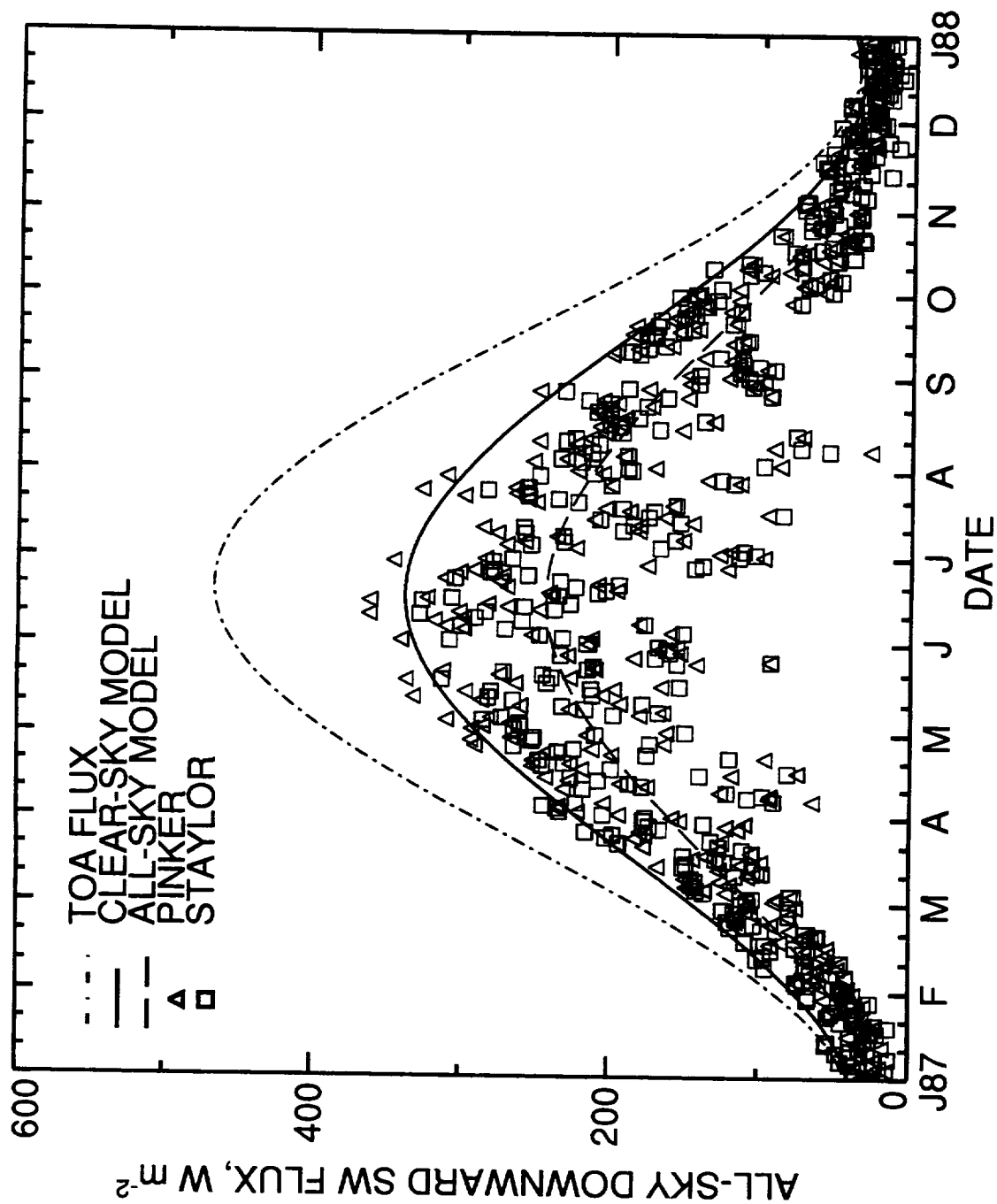


Figure 46. Clear-sky, all-sky and TOA monthly downward SW flux compared to Pinker and Staylor daily all-sky results for the Southern Study Area.

REPORT DOCUMENTATION PAGE			Form Approved OMB No. 0704-0188	
Public reporting burden for this collection of information is estimated to average 1 hour per response, including the time for reviewing instructions, searching existing data sources, gathering and maintaining the data needed, and completing and reviewing the collection of information. Send comments regarding this burden estimate or any other aspect of this collection of information, including suggestions for reducing this burden, to Washington Headquarters Services, Directorate for Information Operations and Reports, 1215 Jefferson Davis Highway, Suite 1204, Arlington, VA 22202-4302, and to the Office of Management and Budget, Paperwork Reduction Project (0704-0188), Washington, DC 20503.				
1. AGENCY USE ONLY (Leave blank)	2. REPORT DATE September 1994	3. REPORT TYPE AND DATES COVERED Technical Memorandum		
4. TITLE AND SUBTITLE Satellite Estimates of Shortwave Surface Radiation and Atmospheric Meteorology for the BOREAS Experiment Region			5. FUNDING NUMBERS 578-12-23-70	
6. AUTHOR(S) C. D. Moats, C. H. Whitlock, S. R. LeCroy, and R. C. DiPasquale				
7. PERFORMING ORGANIZATION NAME(S) AND ADDRESS(ES) NASA Langley Research Center Hampton, VA 23681-0001			8. PERFORMING ORGANIZATION REPORT NUMBER	
9. SPONSORING / MONITORING AGENCY NAME(S) AND ADDRESS(ES) National Aeronautics and Atmospheric Administration Washington, DC 20546-0001			10. SPONSORING / MONITORING AGENCY REPORT NUMBER NASA TM-109132	
11. SUPPLEMENTARY NOTES Whitlock: NASA Langley Research Center, Hampton, VA. Moats, LeCroy, and DiPasquale: Lockheed Engineering and Sciences Company, Hampton, VA.				
12a. DISTRIBUTION / AVAILABILITY STATEMENT Unclassified-Unlimited Subject Category 47			12b. DISTRIBUTION CODE	
13. ABSTRACT (Maximum 200 words) This report provides background data for the Boreal Ecosystem Atmosphere Study (BOREAS) sites, including daily, seasonal, interannual, and spatial variability of shortwave (SW) radiation at the Earth's surface. This background data, from the Version 1.1 SW data set, was provided by the Surface Radiation Budget (SRB) Climatology Project established by the World Climate Research Program (WCRP).				
14. SUBJECT TERMS Surface Radiation ISCCP ERBE Clouds Climate WCRP GEWEX ISLSCP BOREAS			15. NUMBER OF PAGES 56 16. PRICE CODE A04	
17. SECURITY CLASSIFICATION OF REPORT UNCLASSIFIED	18. SECURITY CLASSIFICATION OF THIS PAGE UNCLASSIFIED	19. SECURITY CLASSIFICATION OF ABSTRACT UNCLASSIFIED	20. LIMITATION OF ABSTRACT UL	